Speleogenesis and scallop formation and demise under hydraulic control and other recharge regimes

Article *in* Cave and Karst Science · December 2013

CITATIONS
6

READS
122

1 author:

Trevor Faulkner
University of Birmingham
109 PUBLICATIONS **220** CITATIONS

SEE PROFILE

Cave and Karst Science, Vol.40, No.3, 2013
Transactions of the British Cave Research Association

ISSN 1356-191X

Speleogenesis and scallop formation and demise under hydraulic control and other recharge regimes.

Trevor FAULKNER
Limestone Research Group, Geography, Earth and Environmental Sciences, University of Birmingham, Edgbaston, Birmingham, B15 2TT, UK.

e-mail: trevor@marblecaves.org.uk

Abstract: It is commonly stated in the literature that, as a phreatic conduit enlarges in limestone under hydraulic (constant head) control, the chemical 'breakthrough' point occurs at an exit size of the order of one centimetre at the transition from slow high-order to fast first-order dissolution kinetics. This is commonly assumed to coincide with the change from a wholly laminar flow to the onset of transitional turbulent flow at the Reynolds Number (R_e) of 2200 that applies in artificial pipes. These relationships are approximately true for a range of conduit geometries in sub-horizontally bedded strata, including in aquifers with mid-range hydraulic gradients of 10^{-4} to 10^{-2}. However, the conduit size for the onset of turbulence varies with the hydraulic gradient, whereas that for the onset of first-order kinetics varies with the hydraulic ratio, which is the hydraulic gradient divided by the path length. Furthermore, there is no typical R_e at breakthrough, because R_e is then directly proportional to conduit length. The transitions only coincide at the same exit aperture or radius for the dissolutional enlargement of planar fissures or cylindrical tubes of lengths 394m or 620m at 0°C and 288m or 452m at 10°C, at R_e of 2200 and a friction factor of 0.0218 or 0.0291. The actual conduit size depends mainly on the hydraulic gradient. However, karst conduits commonly reach transitional turbulent flow at $R_e < 2200$ and at higher friction factors, reducing all these 'coincidental' lengths. For shorter lengths, breakthrough occurs first and transitional turbulence is soon reached under first-order kinetics. For longer lengths, transitional turbulence occurs first. This reduces the flow velocity and so increases the conduit size needed for breakthrough, which could be delayed significantly, if the effect of enlargement by mechanical erosion or of a reduced diffusion boundary layer is small. Thus, whether conduit length is less or more than the coincidental length may be important for speleogenesis, if existing models become increasingly invalid for longer lengths at low hydraulic gradients. Conduit sizes for breakthrough and transitional turbulence can be sub-millimetre for short and steep conduits, with $R_e < 10$ at breakthrough, but over a metre for long and shallow conduits, with $R_e > 50{,}000$ at breakthrough. After breakthrough, phreatic conduit enlargement under constant head conditions would continue at the applicable maximum rate as flow rates and velocities increase without limit.

Scallops form on cave walls in fully turbulent flow at $R_e \geq 24{,}860$ by dissolution under fast first-order kinetics, with a maximum observable length of c. 200cm. Speleogenesis under hydraulic control passes through stages of: laminar flow with slow high-order dissolution kinetics; transitional turbulent flow before or after chemical breakthrough; and fully turbulent flow with the probable formation of wall scallops. These reduce in size as the flow velocity increases until they disappear at c. 1cm length, when mechanical erosion dominates over chemical dissolution. The evolution of a conduit after the onset of constant and then reducing recharge conditions depends on whether it continuously descends (when the flow immediately becomes vadose) and on its shape if it forms phreatic loops. The morphology of a vadose canyon indicates whether the transition from phreatic flow occurred at constant recharge, gradually reducing recharge, or suddenly reducing recharge. In phreatic loops under constant recharge, planar fissures become locked into their new flow and chemical regimes at a constant R_e, until they become more circular; their continuing widening is balanced by reducing velocity, which also causes scallop lengths to increase. However, cylindrical tubes under constant recharge and all conduits under reducing recharge immediately start to reverse back through their previous flow regimes towards laminar flow as flow velocity reduces and scallop lengths increase. Synchronously, they also reverse back to high-order dissolution kinetics via the 'limiting recharge point'. If recharge ceases, the outcome is a continuously descending relict passage or a static perched sump, which may dry out by evaporation to create a relict phreatic loop. This paper analyses these relationships and conditions and then discusses their relevance to the multitude of possible natural and artificial karst hydrogeological situations, where hydraulic ratios can be considered over 17 orders of magnitude.

Keywords: Breakthrough, dissolution, hydrogeological, kinetics, laminar, phreatic, recharge, relict, Reynolds Number, scallop, speleogenesis, turbulent, vadose.

Received: 03 November 2013; Accepted 23 December 2013

The physics and chemistry of limestone dissolution in closed phreatic and constant head conditions along planar fissures and cylindrical conduits were derived in two key papers over twenty years ago by Dreybrodt (1990) and Palmer (1991). These built on important earlier works, including those by Weyl (1958), Bögli (1964), White (1977), Plummer et al. (1978) and Palmer (1981). A later treatise to present detailed (and animated) models of speleogenesis based on the principles of the Palmer / Dreybrodt model is that by Dreybrodt *et al*., (2005). Palmer (1991: Eq.6) showed that when water flows past any point in a conduit in natural limestone, the rate of dissolutional wall retreat $S = 31.56k_n(1/\rho)(1 - C/C_s)^n$ cm per year, where k_n mg-cm litre^{-1}s^{-1} is the appropriate reaction coefficient, ρ gm cm^{-3} is the density of the limestone, C gm cm^{-3} is the point concentration of calcite in solution, C_s gm cm^{-3} is the appropriate saturation concentration of calcite and n is the reaction order. k_n, C and C_s vary with temperature and P_{CO2} levels. $k_{n>1}$ also varies with C/C_s, and C also varies with the hydrogeological parameters of the conduit. Dissolution when the solution is well below saturation occurs at a fast 'first-order kinetics' rate, where n = 1. At the beginning of the conduit, C is at a minimum (C_0), and may be close to zero for an allogenic stream running from non-carbonate rocks. In this case, dissolution at the entrance is at the appropriate maximum rate of $S_{max} = 31.56k_1/\rho$ cm a^{-1}. The calcite concentration increases downstream from the entry point. If C approaches C_s, the dissolution rate reduces sharply, some way before a point along the conduit that Weyl (1958) called the 'penetration length', beyond which further dissolution then seemed to be impossible. However, White (1977) showed that, downstream of this "kinetic trigger", the reaction rate remains non-zero, so that the conduit continues to enlarge slowly along its whole length.

Expression	Explanation	Unit	Reference
b	Breadth of a planar fissure	cm	
C	Point concentration of calcite in solution	gram cm^{-3}	
C_0	Initial concentration of calcite in solution. $C_0 = 0$ is assumed herein.	gram cm^{-3}	
C_s	Saturation concentration of calcite	gram cm^{-3}	Palmer (1991)
D-W	Darcy-Weisbach equation: $V^2 = 4(w \text{ or } r)\gamma i/f$ (fissures or tubes)		Palmer (1991: Eq.4)
f	Friction factor	dimensionless	
f_T	Friction factor at the onset of transitional turbulence. $f_T = 0.0218$ (planar fissures) or 0.0291 (tubes) in artificial pipes, if R_{eT} =2200. ≥ 0.02 in karst.	dimensionless	
g = 981	Gravitational acceleration	cm s^{-2}	
gm	gram		
H	Hydraulic Head	m	
H-P	Hagen-Poiseuille equation: $V = (w^2 \text{ or } r^2)\rho g i/(12 \text{ or } 8)\mu$ (fissures or tubes)		Palmer (1991: Eq.3)
i	Hydraulic Gradient = H/L	dimensionless	
i/L	Hydraulic Ratio = H/L^2	m^{-1}	Dreybrodt (1990)
k_n	Coefficient for dissolution reaction of order n	mg-cm litre^{-1}s^{-1}	Palmer (1991)
L	Length of a single karst conduit: planar fissure or cylindrical tube	m	
mg	milligram		
n	Reaction order	dimensionless	Palmer (1991)
Q	Volumetric flow rate = bwV (fissure) or $\pi r^2 V$ (tube)	cm^{3}s^{-1} or litres s^{-1} or m^{3}s^{-1}	
R_e	Conduit flow Reynolds Number = $w\rho V/\mu$ (fissure) or $2r\rho V/\mu$ (tube)	dimensionless	
R_{eT}	Conduit flow R_e at the onset of transitional turbulence. R_{eT} = 2200 in artificial pipes and ≤ 2200 in karst conduits	dimensionless	Kaufmann and Braun (1999)
R_{eB}	Conduit flow R_e at chemical breakthrough = constant x L at any i	dimensionless	Faulkner (2006a)
R_{eF}	Conduit flow R_e when flow reaches full turbulence and wall scallops can start to form. R_{eF} ≤ 30,360 (fissure) or 24,860 (tube)	dimensionless	This paper
R_{eM}	Conduit flow Reynolds Number at V_M	dimensionless	
R_e'	The 'stable flute Reynolds Number' = $\rho V\lambda/\mu$. This is not constant, but if $w=7.6\lambda$ or $r=6.2\lambda$, R_e' = 22,500	dimensionless	Curl (1966)
$R_{e\lambda}$	The scallop Reynolds Number = $\rho V_\lambda \lambda/\mu$ = c. 21,000	dimensionless	Curl (1974)
S	Solutional wall retreat rate. S_{max} = c. 1mm a^{-1} at 10°C and 1% P_{CO2}.	mm a^{-1} or cm a^{-1}	Palmer (1991)
T_B	Breakthrough time: the time taken for flow in an initial planar fissure or cylindrical tube to achieve first-order dissolution kinetics at its exit	years or a	Dreybrodt (1990); Palmer (1991: t_{max})
V	Mean flow velocity	cm s^{-1}	
V_F	Mean flow velocity for the onset of full turbulence	cm s^{-1}	
V_M = c. 300	Minimum mean flow velocity for mechanical erosion to erode scallops	cm s^{-1}	Palmer (2007: 147–149)
V_λ	Mean flow velocity at λ cm 'above' the scallops	cm s^{-1}	Curl (1974)
w or r	Aperture width of a planar fissure or radius of a cylindrical tube	cm	
w_T or r_T	Aperture or radius at the onset of transitional turbulence	cm	
w_B or r_B	Aperture or radius at chemical breakthrough, when dissolution achieves first-order kinetics	cm	
w_F or r_F	Aperture or radius at full turbulence, when wall scallops can start to form	cm	
w_F' or r_F'	Aperture or radius at full turbulence, if previous flow is assumed to be laminar	cm	
w_M or r_M	Aperture or radius when $V = V_M$	cm	Palmer (2007: 147–149)
λ	Length of a wall scallop	cm	Curl (1966)
$\lambda_F = w_F/2$ or r_F	Initial length of a wall scallop when flow reaches full turbulence, up to a maximum of c. 200cm at a minimum V of c. 1cm s^{-1}	cm	Curl (1966); Palmer (2007: 147–149)
λ_M = c. 1cm	Minimum length of a wall scallop when $V = V_M$	cm	Palmer (2007: 147–149)
μ	Dynamic viscosity of water = 0.01793 at 0°C and 0.01307 at 10°C	gram cm^{-1}s^{-1}	Ford and Williams (2007: p.112)
ρ	Density of water or limestone; ρ = 1.000 for water at 0°C and 10°C	gram cm^{-3}	

Expressions used in the text *(the units are those used in the citations).*

The Palmer / Dreybrodt model calculates that the kinetic trigger occurs when $0.6 < C/C_S < 0.9$, dependent on temperature and P_{CO2}. The downstream reaction proceeds with slow 'high-order kinetics' with $n \geq 4$, its rate being governed by non-calcitic impurities. The continuing dissolutional enlargement causes the flow rate to increase slowly, which reduces the calcite concentration along the conduit, so that the penetration length also slowly increases. When the exit aperture is large enough, dissolution at the applicable first-order S_{max} rate reaches the exit, and dissolution then occurs at this fast rate along the whole length of the flow path, to create a conduit with a near-uniform cross-section. This important event in karst evolution is called the "breakthrough point" (Dreybrodt, 1990), which commonly occurs rather abruptly. If limestone comprised pure calcite, the penetration length might not increase and caves would then only form if initial fracture geometries allowed immediate first-order dissolution kinetics along the whole conduit, i.e. 'tectonic inception' (Faulkner, 2006a; 2006b). At 10°C and with the inflowing water equilibrating with soil-air containing 1% CO_2, S_{max} = c. 1mm per year (Palmer, 1991), although dissolution rates faster by an order of magnitude seem possible in water that is extremely unsaturated (e.g. Palmer, 1991: Fig.8; Kaufmann, 2003). Wall retreat rates may also be increased in turbulent flow by mechanical erosion, which is lithology dependent, but not easy to quantify. Thus, fast first-order kinetics apply especially at high flow rates and low calcite concentrations, in karst systems with high flow velocities, short flow-through times, large hydraulic gradients and with large and/or short conduits. During Quaternary timescales, dissolution can commonly be regarded as either 'on' at an appropriate S_{max} rate or 'off'. For all carbonate dissolutional speleogenesis, it is the reaction rate (i.e. the dissolution rate, chemical erosion rate or wall retreat rate, S) and the process time available that are important for passage enlargement, not the solubility (i.e. the saturation or equilibrium concentration, which equals the maximum amount of carbonate that can be dissolved), although both depend on the temperature and P_{CO2} levels. Prior to the derivations of the Palmer / Dreybrodt model, this distinction was not always recognized, leading to considerable confusion about the process of karstification, as discussed by Faulkner (2009a).

White (1977) pointed out that the change to fast dissolution can occur at an exit aperture of 1–10mm, and Dreybrodt (1990: p.645) suggested 1–10cm for this breakthrough, ranges that have been widely quoted. White (1977) also stated that this coincides approximately with the size at which wholly laminar flow starts to become turbulent (without there being a causal relationship), and this "coincidence" at chemical breakthrough has also been widely assumed. Chemical breakthrough has even been redefined as the onset of turbulence (Hanna and Rajaram, 1998). Karst hydrologists record that hydraulic gradients commonly occur in the range 10^{-4} to 10^{-2} for karst aquifers in sub-horizontal sedimentary limestones (e.g. White, 1988: p.165). This paper analyses these relationships, amplifying preliminary studies (Faulkner, 2006a, 2013), and integrates the Palmer / Dreybrodt model with the theory of scallop formation (Curl, 1966, 1974) and scallop demise. The analysis commonly studies flows in both planar fissures and cylindrical tubes at both 0°C and 10°C. This provides relevance to a multitude of karst hydrogeological situations, from chemical and tectonic inception at low and high hydraulic gradients to large discharges from large conduits, both in deglacial/alpine and in temperate environments. Spreadsheet calculations have commonly been reduced to three significant figures.

Hydraulic gradient and hydraulic ratio

Flow rates, water velocities and the change from laminar to transitional turbulent flow in conduits are controlled by the hydraulic gradient (i: Head/path length = H/L) and the Reynolds Number (R_e: see below), among other less important variables. The main parameters at the chemical breakthrough point are controlled by a geometrical variable called the "hydraulic ratio", which equals the hydraulic gradient divided by the path length (i/L; Dreybrodt, 1996). The necessity for the extra divisor can be understood, because dissolution always proceeds along the whole path length. Hence, if the onsets of transitional turbulence and first-order kinetics occur at the same conduit size, that must be coincidental. Based on the work of Palmer (1991), which itself was based on the Hagen-Poiseuille (H-P) equation for laminar flow, the relationships required to achieve first-order dissolution kinetics were plotted graphically by Faulkner (2006a: Fig.3). Those curves illustrated the linear relationships among the logarithms of hydraulic conductivity, mean water velocity, volumetric flow rate, hydraulic ratio and the exit apertures at the breakthrough point for both wide planar fissures and circular tubes of lengths 1–1000m, with their applicable R_e values. However, wholly laminar flow prior to breakthrough was assumed for all these cases.

Onset of transitional turbulent flow

Dimensionless Reynolds Numbers are used to characterize flow regimes in fissures or pipes. These are commonly, but not consistently, defined as: $R_e = w\rho V/\mu$ (planar fissures: Dreybrodt *et al*., 2005; not dependent on b, the fissure breadth, if b >> w) or $R_e = 2r\rho V/\mu$ (cylindrical tubes: Kaufmann and Braun, 1999; Ford and Williams, 2007, p.109), where (w or r) = aperture width or radius in cm, ρ = the density of the water in gm cm^{-3}, V = its mean velocity in cm s^{-1} and μ = its dynamic viscosity in gm $cm^{-1}s^{-1}$. Laminar flows in fissures or tubes under hydraulic control (constant head) obey the H-P equation: $V = (w^2 \text{ or } r^2)\rho gi/(12 \text{ or } 8)\mu$, by re-arrangement of Palmer (1991: Eq.3), where g is the gravitational acceleration in cm s^{-2}. Normally, $0 \leq i \leq 1$, where i = 1 is the normal maximum for vertical flow paths under subaerial conditions. However, i > 1 is possible for inlets submerged beneath a deep river, reservoir or lake, if the outlet is in a lower valley. The above equations can be re-arranged to state the applicable aperture or radius in terms of R_e:

$$(w \text{ or } r) = ((12 \text{ or } 4)R_e\mu^2/\rho^2 gi)^{1/3} \quad \textbf{[1]}$$

The volumetric flow rate $Q = bwV = bR_e\mu/\rho$ (for fissures) or $Q = \pi r^2 V = \pi r R_e \mu/2\rho$ (for tubes). The value of R_{eT} at which flows in straight artificial pipes commonly move into transitional turbulence is 2200 and Kaufmann and Braun (1999, p.3229) used this value for "smooth turbulence" in their treatment for karst aquifer evolution. This is the point at which small eddies build up near the conduit wall. However, in irregular and tortuous cave conduits, an induced turbulence can arise at $R_{eT} << 2200$. R_e can be derived for flow regimes along completely flooded, but surveyed, cave passages. However, R_e remains unknown for small inaccessible cave conduits of unknown size, although it should be possible to devise experiments using artificial slots and tubes in blocks of limestone to provide some constraints on R_{eT}. Nevertheless, the value of $R_{eT} = 2200$ is used in the following calculations at all applicable temperatures for both conduit cross-section shapes, with the caveat that this is probably the maximum value that can apply. Thus, substituting R_{eT} and the given constants for fissures or tubes into the equations above gives:

$$(w_T \text{ or } r_T) = (0.205 \text{ or } 0.142)/i^{1/3} \text{ cm at } 0°C \quad \textbf{[2]}$$
$$(w_T \text{ or } r_T) = (0.166 \text{ or } 0.115)/i^{1/3} \text{ cm at } 10°C \quad \textbf{[2]}$$
$$Q_T = (39.4b \text{ or } 62.0r_T) \text{ cm}^3\text{s}^{-1} \text{ at } 0°C$$
$$Q_T = (28.8b \text{ or } 45.2r_T) \text{ cm}^3\text{s}^{-1} \text{ at } 10°C$$

Therefore, (w_T or r_T) for the onsets of transitional turbulent flow vary with temperature (which determines the viscosity), cross-section shape and the inverse of the cube root of i, but are independent of conduit length for uniform conduits at each hydraulic gradient. These relationships at 10°C are presented in Table 1 and illustrated with logarithmic scales in Figure 1 (fissures) or Figure 2 (tubes) by the lowest dashed lines. These plot lines show how the conduit sizes for the onset of transitional turbulent flow reduce as the hydraulic gradient of the conduit increases. These conduit sizes vary from (166 or 115)cm at $i = 10^{-9}$ via (0.17 or 0.12)cm at $i = 10^0$ (vertical) to (0.008 or 0.005)cm at $i = 10^4$. The slope of the dashed lines = -0.333 log cm per log i.

All turbulent flows in fissures or tubes obey the Darcy-Weisbach (D-W) equation: $V^2 = 4(w \text{ or } r)gi/f$ for fissures or tubes, so that $(w \text{ or } r) = V^2 f/4gi$, by re-arrangement of Palmer (1991: Eq.4), where f is a dimensionless friction factor that depends only on the conduit geometry. In cave studies, it represents both head losses caused by bends, corners and changes in cross-section and by the roughness of conduit projections relative to conduit size.

Substituting V from the Reynolds equation:

$$(w \text{ or } r) = V^2 f/4gi = (R_e\mu/((w \text{ or } 2r)\rho))^2/4gi$$
$$= (R_e^2\mu^2 f/(4 \text{ or } 16)\rho^2 gi)^{1/3} \quad \textbf{[3]}$$

At the onset of transitional turbulence, the H-P and D-W values of (w_T or r_T) in **[1]** and **[3]** are equal, giving the applicable friction factor $f_T = 48/R_{eT}$ (fissure) or $f_T = 64/R_{eT}$ (tube). Thus, for karst conduits at the onset of transitional turbulence, if $R_{eT} = 2200$, $f_T = 0.0218$ or $f_T = 0.0291$, at any temperature. However, higher friction factors >0.1, or even >100

Length L	Head H	Hydraulic gradient i H/L	Fissure aperture w_T $0.1663/i^{⅓}$	Tube radius r_T $0.1153/i^{⅓}$	Hydraulic ratio i/L H/L^2	log w_B = −(4.7957+ log(i/L))/3	Fissure aperture w_B $0.0252/(i/L)^{⅓}$	log r_B = −(5.4689+ log(i/L))/3	Tube radius r_B $0.0150/(i/L)^{⅓}$	Ratio w_T/w_B	Ratio r_T/r_B
m	m	-	cm	cm	m^{-1}	log cm	cm	log cm	cm	-	-
10000	0.00001	1.00E-09	166.1907	115.2344	1.00E-13	2.7348	542.9585	2.5104	323.8670	0.31	0.36
1000	0.00001	1.00E-08	77.1448	53.4912	1.00E-11	2.0681	116.9769	1.8437	69.7750	0.66	0.77
100	0.00001	1.00E-07	35.8102	24.8303	1.00E-09	1.4014	25.2019	1.1770	15.0326	1.42	1.65
10	0.00001	1.00E-06	16.6229	11.5261	1.00E-07	0.7348	5.4296	0.5104	3.2387	3.06	3.56
1	0.00001	1.00E-05	7.7163	5.3503	1.00E-05	0.0681	1.1698	-0.1563	0.6978	6.60	7.67
10000	0.0001	1.00E-08	77.1448	53.4912	1.00E-12	2.4014	252.0190	2.1770	150.3257	0.31	0.36
1000	0.0001	1.00E-07	35.8102	24.8303	1.00E-10	1.7348	54.2959	1.5104	32.3867	0.66	0.77
100	0.0001	1.00E-06	16.6229	11.5261	1.00E-08	1.0681	11.6977	0.8437	6.9775	1.42	1.65
10	0.0001	1.00E-05	7.7163	5.3503	1.00E-06	0.4014	2.5202	0.1770	1.5033	3.06	3.56
1	0.0001	1.00E-04	3.5818	2.4836	1.00E-04	-0.2652	0.5430	-0.4896	0.3239	6.60	7.67
10000	0.001	1.00E-07	35.8102	24.8303	1.00E-11	2.0681	116.9769	1.8437	69.7750	0.31	0.36
1000	0.001	1.00E-06	16.6229	11.5261	1.00E-09	1.4014	25.2019	1.1770	15.0326	0.66	0.77
100	0.001	1.00E-05	7.7163	5.3503	1.00E-07	0.7348	5.4296	0.5104	3.2387	1.42	1.65
10	0.001	1.00E-04	3.5818	2.4836	1.00E-05	0.0681	1.1698	-0.1563	0.6978	3.06	3.56
1	0.001	1.00E-03	1.6627	1.1529	1.00E-03	-0.5986	0.2520	-0.8230	0.1503	6.60	7.67
10000	0.01	1.00E-06	16.6229	11.5261	1.00E-10	1.7348	54.2959	1.5104	32.3867	0.31	0.36
1000	0.01	1.00E-05	7.7163	5.3503	1.00E-08	1.0681	11.6977	0.8437	6.9775	0.66	0.77
100	0.01	1.00E-04	3.5818	2.4836	1.00E-06	0.4014	2.5202	0.1770	1.5033	1.42	1.65
10	0.01	1.00E-03	1.6627	1.1529	1.00E-04	-0.2652	0.5430	-0.4896	0.3239	3.06	3.56
1	0.01	1.00E-02	0.7718	0.5352	1.00E-02	-0.9319	0.1170	-1.1563	0.0698	6.60	7.67
10000	0.1	1.00E-05	7.7163	5.3503	1.00E-09	1.4014	25.2019	1.1770	15.0326	0.31	0.36
1000	0.1	1.00E-04	3.5818	2.4836	1.00E-07	0.7348	5.4296	0.5104	3.2387	0.66	0.77
100	0.1	1.00E-03	1.6627	1.1529	1.00E-05	0.0681	1.1698	-0.1563	0.6978	1.42	1.65
10	0.1	1.00E-02	0.7718	0.5352	1.00E-03	-0.5986	0.2520	-0.8230	0.1503	3.06	3.56
1	0.1	1.00E-01	0.3583	0.2484	1.00E-01	-1.2652	0.0543	-1.4896	0.0324	6.60	7.67
10000	1	1.00E-04	3.5818	2.4836	1.00E-08	1.0681	11.6977	0.8437	6.9775	0.31	0.36
1000	1	1.00E-03	1.6627	1.1529	1.00E-06	0.4014	2.5202	0.1770	1.5033	0.66	0.77
100	1	1.00E-02	0.7718	0.5352	1.00E-04	-0.2652	0.5430	-0.4896	0.3239	1.42	1.65
10	1	1.00E-01	0.3583	0.2484	1.00E-02	-0.9319	0.1170	-1.1563	0.0698	3.06	3.56
1	1	1.00E+00	0.1663	0.1153	1.00E+00	-1.5986	0.0252	-1.8230	0.0150	6.60	7.67
10000	10	1.00E-03	1.6627	1.1529	1.00E-07	0.7348	5.4296	0.5104	3.2387	0.31	0.36
1000	10	1.00E-02	0.7718	0.5352	1.00E-05	0.0681	1.1698	-0.1563	0.6978	0.66	0.77
100	10	1.00E-01	0.3583	0.2484	1.00E-03	-0.5986	0.2520	-0.8230	0.1503	1.42	1.65
10	10	1.00E+00	0.1663	0.1153	1.00E-01	-1.2652	0.0543	-1.4896	0.0324	3.06	3.56
1	10	1.00E+01	0.0772	0.0535	1.00E+01	-1.9319	0.0117	-2.1563	0.0070	6.60	7.67
10000	100	1.00E-02	0.7718	0.5352	1.00E-06	0.4014	2.5202	0.1770	1.5033	0.31	0.36
1000	100	1.00E-01	0.3583	0.2484	1.00E-04	-0.2652	0.5430	-0.4896	0.3239	0.66	0.77
100	100	1.00E+00	0.1663	0.1153	1.00E-02	-0.9319	0.1170	-1.1563	0.0698	1.42	1.65
10	100	1.00E+01	0.0772	0.0535	1.00E+00	-1.5986	0.0252	-1.8230	0.0150	3.06	3.56
1	100	1.00E+02	0.0358	0.0248	1.00E+02	-2.2652	0.0054	-2.4896	0.0032	6.60	7.67
10000	1000	1.00E-01	0.3583	0.2484	1.00E-05	0.0681	1.1698	-0.1563	0.6978	0.31	0.36
1000	1000	1.00E+00	0.1663	0.1153	1.00E-03	-0.5986	0.2520	-0.8230	0.1503	0.66	0.77
100	1000	1.00E+01	0.0772	0.0535	1.00E-01	-1.2652	0.0543	-1.4896	0.0324	1.42	1.65
10	1000	1.00E+02	0.0358	0.0248	1.00E+01	-1.9319	0.0117	-2.1563	0.0070	3.06	3.56
1	1000	1.00E+03	0.0166	0.0115	1.00E+03	-2.5986	0.0025	-2.8230	0.0015	6.60	7.67
10000	10000	1.00E+00	0.1663	0.1153	1.00E-04	-0.2652	0.5430	-0.4896	0.3239	0.31	0.36
1000	10000	1.00E+01	0.0772	0.0535	1.00E-02	-0.9319	0.1170	-1.1563	0.0698	0.66	0.77
100	10000	1.00E+02	0.0358	0.0248	1.00E+00	-1.5986	0.0252	-1.8230	0.0150	1.42	1.65
10	10000	1.00E+03	0.0166	0.0115	1.00E+02	-2.2652	0.0054	-2.4896	0.0032	3.06	3.56
1	10000	1.00E+04	0.0077	0.0054	1.00E+04	-2.9319	0.0012	-3.1563	0.0007	6.60	7.67

Table 1: *Fissure and tube sizes for the onsets of transitional turbulence at R_{eT} = 2200 and first-order kinetics at 10°C for various lengths and hydraulic gradients.*

(Palmer, 1991, 2007), can apply for tortuous karst conduits, where R_{eT} << 2200 at the onset of turbulence. Because increasing f reduces R_{eT}, and therefore (w_T or r_T), flows in enlarging karst conduits with higher friction factors become non-laminar earlier.

Onset of first-order kinetics

The approximate fissure aperture w_B or tube radius r_B at the breakthrough point at 10°C with 1% P_{CO2} for an unsaturated input stream (i.e. $C_0 = 0$) in laminar flow under constant head conditions were derived by Faulkner (2006a) from the discussion by Palmer (1991: p.8 and Figs 12a and 12b). These gave:

$\log w_B = \log r_B = -(5+\log(i/L))/3$ log cm,

where i/L m^{-1} = the hydraulic ratio and the path length L is measured in metres.

However, more accurate derivations can be based on the statement that S_{max} is "achieved when Q/rL or Q/bL exceeds 0.001 cm/s" (Palmer, 1991, p.8, where L is measured in cm). From the H-P equation for fissures or tubes, at breakthrough (where L is measured in metres):

$Q_B = 0.1(b \text{ or } r_B)L$ cm^3 s^{-1},

$V_B = 0.1L/(w_B \text{ or } \pi r_B) = (w_B^2/12 \text{ or } r_B^2/8)\rho g i/\mu$ cm s^{-1}

Hence,

$(w_B \text{ or } r_B) = ((1.2 \text{ or } 0.8/\pi)\mu L/\rho g i))^{⅓}$ cm **[4]**

$(w_B \text{ or } r_B) = (0.0280 \text{ or } 0.0167)/(i/L)^{⅓}$ cm at 0°C

$(w_B \text{ or } r_B) = (0.0252 \text{ or } 0.0150)/(i/L)^{⅓}$ cm at 10°C

$\log(w_B \text{ or } r_B) = -((4.66 \text{ or } 5.33) + \log(i/L))/3$ log cm at 0°C

$\log(w_B \text{ or } r_B) = -((4.80 \text{ or } 5.47) + \log(i/L))/3$ log cm at 10°C

Thus, the conduit sizes for the chemical breakthrough point vary with temperature, cross-section shape and the inverse of the cube root of hydraulic ratio, i.e. they increase as i reduces and as L increases. It is assumed that dissolution does not increase b, the fissure breadth. From the Reynolds equation for fissures or tubes at breakthrough:

$R_{eB} = (w_B \text{ or } 2r_B)\rho V/\mu = (0.1 \text{ or } 0.2/\pi)L\rho/\mu$

$R_{eB} = (5.58 \text{ or } 3.55)L$ at 0°C

$R_{eB} = (7.65 \text{ or } 4.87)L$ at 10°C

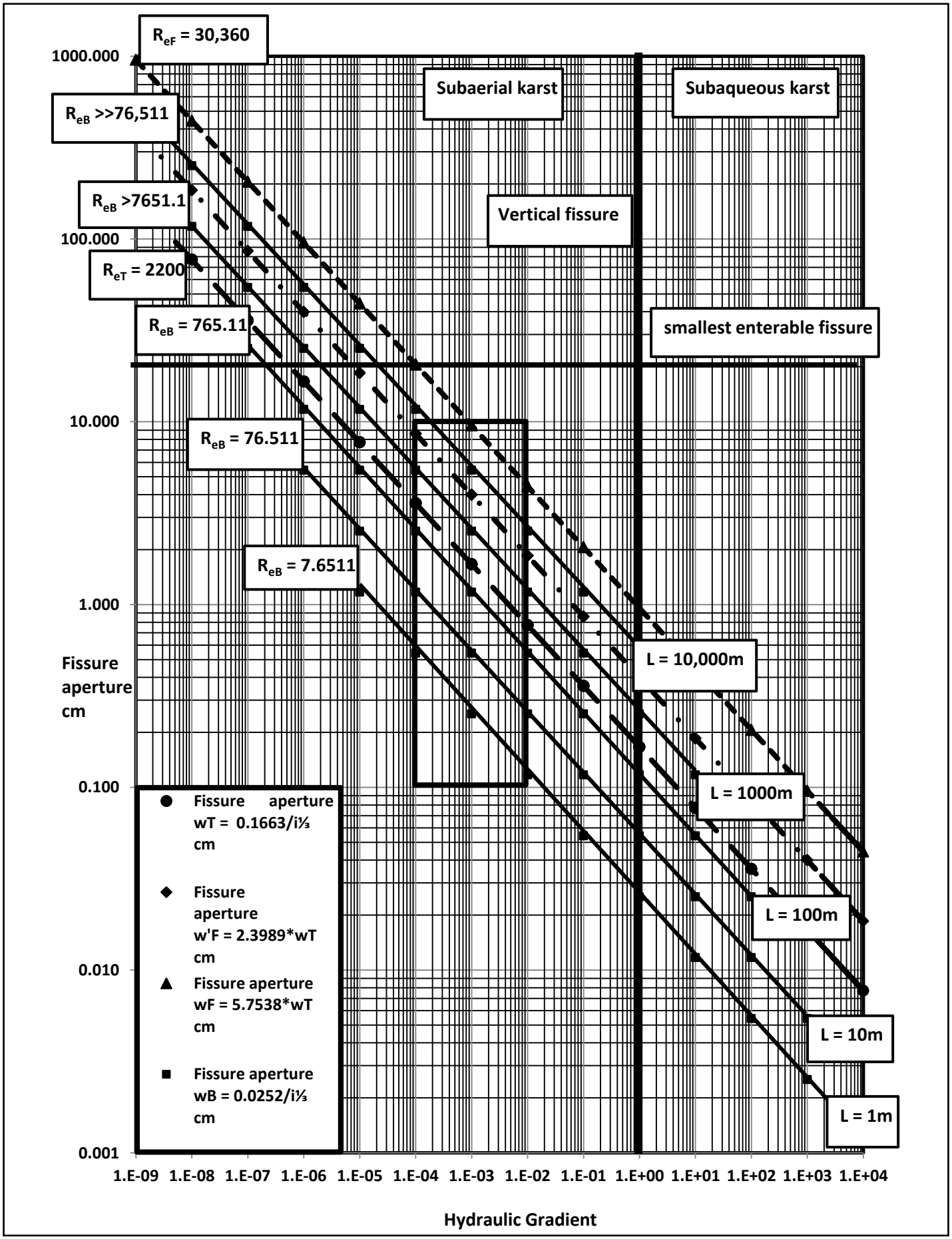

Figure 1: *Minimum planar fissure aperture (w_T, w_F or w_B) in cm for the onset of transitionally and fully turbulent flow at R_e = 2200 and 30,360 or for first-order dissolution kinetics at breakthrough at 10°C and 1% P_{CO2}, plotted against hydraulic gradient (i). The three dashed lines (for w_T, w_F' and w_F) are independent of path length. The middle and upper dashed lines for w_F' and w_F are drawn as if the H-P equation or the D-W equation apply prior to full turbulence. w_B (solid lines) are shown correctly for path lengths of 1m, 10m and 100m. w_B for 1000m and 10,000m are drawn as if the H-P equation applies before breakthrough, despite being longer than the coincidental length. The boxed area covers i from 10^{-4} to 10^{-2} and conduit sizes from 1mm to 10cm. The vertical line indicates the maximum i of 1, for vertical flow paths under normal subaerial conditions. For karst submerged by a reservoir or lake, i can be >1. The horizontal line indicates the smallest conduit enterable by a caver. Refer also to the text.*

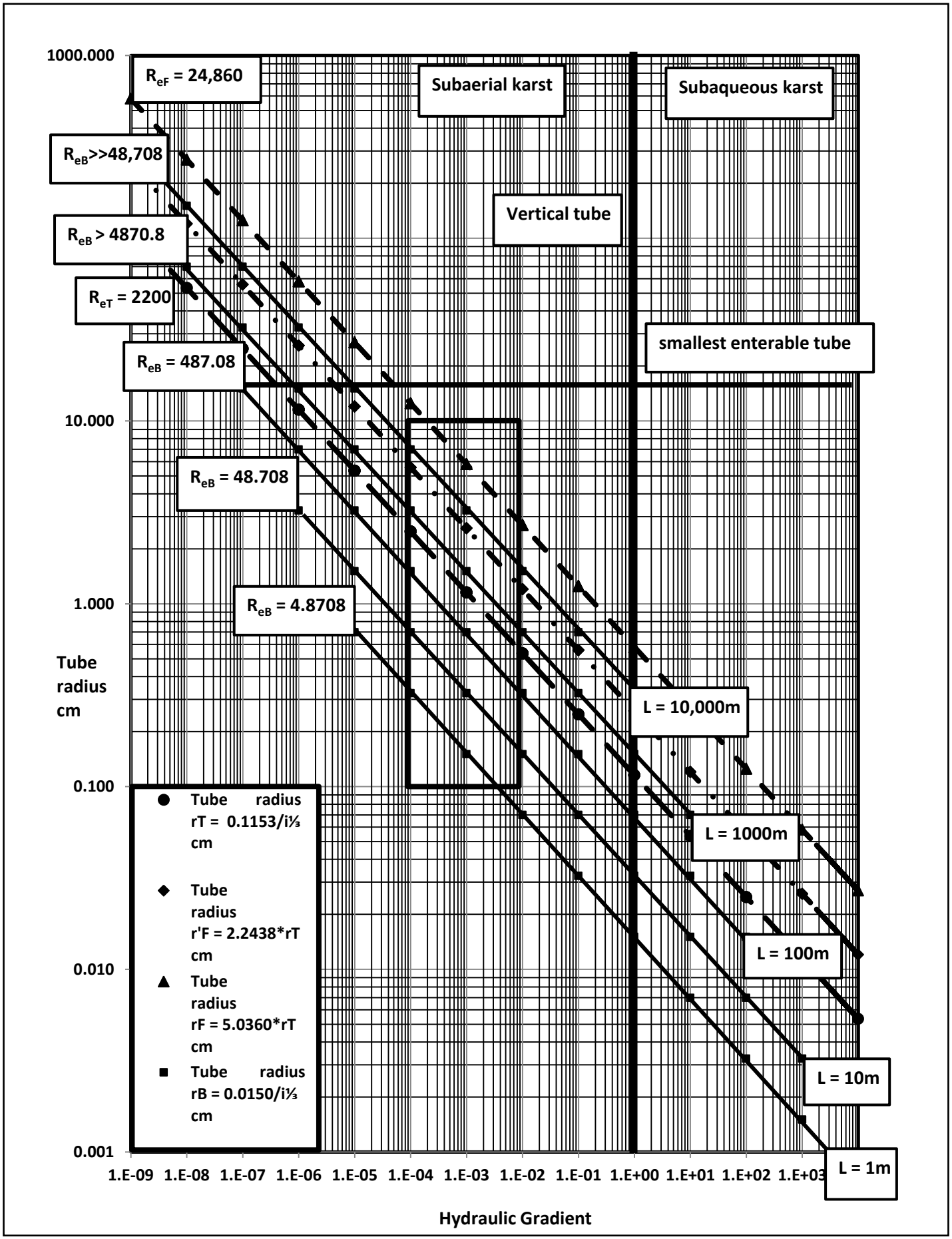

Figure 2: *Minimum radius for a cylindrical tube (r_T, r_F or r_B) in cm for the onset of transitionally and fully turbulent flow at Re = 2200 and 24,860 or for first-order dissolution kinetics at breakthrough at 10°C and 1% P_{CO2}, plotted against hydraulic gradient (i). The three dashed lines (for r_T, r_F' and r_F) are independent of path length. The middle and upper dashed lines for r_F' and r_F are drawn as if the H-P equation or the D-W equation apply prior to full turbulence. r_B (solid lines) are shown correctly for path lengths of 1m, 10m and 100m. r_B for 1000m and 10,000m are drawn as if the H-P equation applies before breakthrough, despite being longer than the coincidental length. The boxed area covers i from 10^{-4} to 10^{-2} and conduit sizes from 1mm to 10cm. The vertical line indicates the maximum i of 1, for vertical flow paths under normal subaerial conditions. For karst submerged by a reservoir or lake, i can be >1. The horizontal line indicates the smallest conduit enterable by a caver. Refer also to the text.*

This shows the important conclusion that, at the transition to first-order kinetics, R_{eB} is directly proportional to the length of the conduit. This contrasts with the transition to turbulent flow in the same conduit (and therefore at the same hydraulic gradient), where R_{eT} is independent of its length. These relationships are also presented for 10°C in Table 1 and illustrated in Figs 1 and 2 by solid lines. These lines show how the conduit sizes for the establishment of first-order kinetics reduce as the hydraulic gradient increases, at five set lengths, L, from 1 – 10,000m and their applicable R_{eB} values. The aperture or radius required for breakthrough at 10°C vary from (543 or 324)cm for a 10km flow route with i = 10^{-9} and i/L = $10^{-13}m^{-1}$ (and R_e = 76,500 or 48,700) via (0.12 or 0.07)cm for a 100m length with i = 10^0 and i/L = $10^{-2}m^{-1}$ (and R_e = 765 or 487) to (0.0012 or 0.0007)cm for a 1m length with i = 10^4 and i/L = 10^4m^{-1} (and R_e = 7.65 or 4.87). However, wholly laminar flow is still assumed prior to breakthrough for all these conduit lengths, which is not necessarily true, as discussed below. The slope of the solid line for each set length = -0.333 log cm per log i, so that these lines are parallel to the lowest dashed lines.

Coincidence and non-coincidence of transitional turbulence and breakthrough

Whether transitional turbulence or chemical breakthrough occurs first during conduit enlargement by dissolution can be determined from the ratios (w_T/w_B or r_T/r_B) for fissures or tubes. Thus from **[1]** and **[4]**:

$(w_T/w_B \text{ or } r_T/r_B) = ((12 \text{ or } 4)R_{eT}\mu^2/\rho^2 gi)^{⅓}/((1.2 \text{ or } 0.8/\pi)\mu L/\rho gi)^{⅓}$

If R_{eT} = 2200 then:

$(w_T/w_B \text{ or } r_T/r_B) = 10((22 \text{ or } 11\pi)\mu/\rho L)^{⅓}$

$(w_T/w_B \text{ or } r_T/r_B) = (7.33 \text{ or } 8.53)/L^{⅓}$ at 0°C

$(w_T/w_B \text{ or } r_T/r_B) = (6.60 \text{ or } 7.67)/L$ at 10°C

These ratios depend on temperature, conduit shape and the inverse of the cube root of the conduit length, but not on the hydraulic gradient, as also shown in Table 1. If $R_{eT} < 2200$, the ratios reduce in proportion to $R_{eT}^{⅓}$. The onsets of transitional turbulent flow and first-order kinetics coincide at the same conduit sizes if the ratios equal unity, giving coincidental lengths at R_{eT} = 2200 of:

L = (394 or 620) m at 0°C and

L = (288 or 452)m at 10°C

for any hydraulic gradient and its related conduit size. At these lengths, the plots of the minimum conduit sizes for breakthrough and first-order kinetics at 10°C would exactly coincide at R_{eT} = 2200 with the lowest dashed lines for the onsets of transitional turbulence shown on Figs 1 and 2. However, these are the longest possible 'coincidental' lengths. If $R_{eT} < 2200$, so that $f_T >$ (0.0218 or 0.0291), the lengths and conduit sizes reduce in proportion to R_{eT} and f_T and to $R_{eT}^{⅓}$ and $f_T^{⅓}$.

For conduits that are shorter than the coincidental lengths at any i, the ratios are >1, so that breakthrough at $R_{eB} < R_{eT}$ is reached before the onset of turbulent flow. Therefore, dissolution then proceeds at the S_{max} rate under fast first-order kinetics in laminar flow and continues at that rate when transitional turbulent flow is reached at the required conduit size at R_{eT}. At the L = 1m short length extreme, the conduit size has to increase by a factor of c. 7 to cause transitional turbulence (Table 1). However, even at a low i of 10^{-5}, a transitionally turbulent tube radius of c. 5cm would take only c. 50 years to be reached if S_{max} = 1mm a^{-1}. For L = 100m at i = 10^{-7}, the c. 10cm required radius increase would still take only c. 100 years. At larger hydraulic gradients, all the delays from breakthrough to transitional turbulence are reduced.

For conduits longer than the coincidental lengths, transitional turbulence starts before breakthrough is achieved at $R_{eB} > R_{eT}$. For each conduit size, turbulence reduces the discharge rate, mean velocity and therefore the penetration length, as calculated by Dreybrodt (1988: Eq.9.12). Because the Palmer / Dreybrodt analysis of breakthrough time applies for laminar flow, the model may become increasingly invalid for long conduits at low hydraulic gradients. Importantly, Palmer (1991: Eq.6) stated that the dissolution rate depends on the chemical regime, (which is determined by the hydraulic ratio) but not on the flow regime, if pH > 4. This also applies if the rate-increasing effect of a thinner diffusion boundary layer (Dreybrodt, 1988, p.175) is negligible during initial transitional turbulence. Hence, for these longer conduits, the onset of first-order dissolution kinetics may be delayed and only achieved at larger aperture sizes and larger R_{eB} values than calculated above and as shown in Table 1 and on Figs 1 and 2. For conduit lengths up to 10,000m, conduit sizes need to increase by factors up to c. 3 after transitional turbulence to achieve breakthrough (Table 1). The delays involved are problematical to estimate: modelling of breakthrough time when high-order dissolution kinetics persist after the onset of turbulent flow has apparently not yet been reported. These delays are discussed further below.

Breakthrough time

Dreybrodt (1990) and Palmer (1991) presented similar equations to represent T_B, the time taken for a planar fissure with an initial aperture of w_0 to achieve chemical breakthrough under hydraulic control. A simplified form of Palmer (1991: Eq.8) is T_B = constant/$(w_0^{3.12}(i/L)^{1.37})$ years, where the constant varies with temperature and the P_{CO2} of the input stream. Palmer (1991: Fig.13) plotted T_B against i/L for various w_0 from 0.001–0.1cm for 1,000,000 ≥ T_B ≥ 100 years. However, from the above analysis, this treatment may be inadequate for conduits much longer than the coincidental length at low hydraulic gradients. Indeed, breakthrough may never occur for very long conduits in either laminar or transitionally turbulent flow within applicable geological timescales, although they could eventually reach large sizes, even under high-order kinetics. For T_B < 100 years, the linear relationships on log-log scales also break down, reaching T_B = 0 for conditions at tectonic inception (Faulkner, 2006a: Fig.5). For such systems that are close to breakthrough at inception, any delays caused by prior turbulence are insignificant.

Interestingly, Hanna and Rajaram (1998) and Gabrovsek (2000) analysed the effects of roughness on T_B in laminar flow by introducing a type of friction factor, as also discussed by Dreybrodt *et al*. (2005: 52–55). It was concluded that T_B can reduce or increase, depending on the assumptions made, such as whether the flow rate is held constant (so that V increases), or is reduced, as roughness increases. However, in all systems under hydraulic control, increasing roughness along a single conduit must reduce the flow rate, and therefore the mean velocity. This is equivalent to reducing i and therefore i/L, and thus it increases T_B.

There is an enormous range of breakthrough times in natural and artificial karst systems that vary with hydraulic ratio and initial aperture. For long and possibly fractured limestone aquifers, the flow route might reach deep below the surface and even pass through non-calcitic lithologies before rising to the resurgence. Because natural fractures tend to reduce in size with depth and the rock temperature increases, the flow would follow a path through apertures of varying initial size at varying temperatures, with the possible addition of strong acid dissolution. The effect on breakthrough times is much more complex. This is the realm of hypogene speleogenesis (Klimchouk, 2007), where this new science still requires considerable analysis and quantification (Faulkner, 2007).

Mixing corrosion

Before breakthrough, the extra dissolutional effect of "mixing corrosion" (Bögli, 1964) can be significant in reducing T_B if sustained over long geological time (Dreybrodt *et al.,* 2005). Mixing corrosion occurs when separate flows of nearly saturated waters mix, if they have differing calcite concentrations. This generates a continuing solution that initially is more aggressive than either input. Such mixing conditions can apply during relatively long flows of meteoric water through karst aquifers and also during deep hypogenic flows. Mixing corrosion could also be important in reducing the delay to breakthrough in flow systems that are longer than the coincidental lengths discussed above. However, well before breakthrough, when C/C_s becomes <90%, "breakthrough behaviour" dominates and mixing corrosion becomes less and less important (Romanov *et al*., 2003).

Scallop formation and the onset of full turbulence

Conduits continue to enlarge by chemical dissolution in transitional turbulent flow under hydraulic control. Kaufmann and Braun (1999: Fig.5) showed (presumably for flow in artificial tubes) that f initially reduces as R_e increases. The friction factor then tends towards a constant value 0.04 at r = 1mm and R_e = c. 50,000, reducing to a minimum of c. 0.01 at r = 10cm and R_e = c. 10^7, when V = 65m s^{-1}, at a volumetric flow rate of 2m^3s^{-1}. These are the points at which full (or "rough") turbulence is reached, where f depends on the conduit roughness, but not on R_e. The relationships between f and R_e are little understood for inaccessible karst conduits, but a common reduction in f as conduit size increases under transitional turbulent flow also seems likely. Nevertheless, f will be held

constant in the following calculations at f_T = (0.0218 or 0.0291) for fissures or tubes, whilst R_e and V increase as the conduit enlarges. A caveat is that, in practice, f_T may be larger, but as the conduit enlarges, f will reduce from a previous maximal value until full turbulence is gained.

Scallops (Figs 3 and 4) form only on the surfaces of cave passages in turbulent flow. The steep sides of scallops point downstream and, perhaps unexpectedly, scallops also migrate downstream (Curl, 1966, 1974). They become over-printed by subsequent flow regimes, slowly reducing in mean length λ as conduit size and flow velocity increase under hydraulic control. Scallops commonly represent a final or a present high-stage velocity at scallop dominant discharge, when observed in relict passages or sumps. Palmer (2007, 147–149) suggested approximate practical scallop length limits of $0.5 < \lambda < 200$cm and that at $V < 1$cm s^{-1}, the velocity is too low for turbulence to create observable scallops, whereas at $V > 300$cm s^{-1}, it is high enough for mechanical erosion by entrained sediments to dominate over scallop formation. It also occurs to this author that high flow velocities could cause significant, but lithology-dependent, mechanical erosion, without an allogenic sediment load. However, such erosion would itself necessarily create an autogenic sediment load.

Based on λ and the mean conduit flow velocity V, Curl (1966: p.127) estimated the "stable flute Reynolds Number" as $R_e' = \rho V\lambda/\mu = 22{,}500$. This gave $\lambda V = 22{,}500\mu/\rho$ = (403 and 294) cm^2s^{-1} at 0°C and 10°C. Subsequently, it was determined more accurately by experiment that the "scallop Reynolds Number" $R_{e\lambda} = \rho V_\lambda \lambda/\mu$ = c. 21,000, where V_λ is the flow velocity at λ cm 'above' the scallops (Blumberg and Curl, 1974; Curl, 1974). This gives λV_λ = (377 and 274) cm^2s^{-1} at 0°C and 10°C and shows that λ is inversely proportional to V_λ and that R_e' and λV are not constant as a conduit enlarges. They derived λ by the Sauter Mean statistical method ($\Sigma\lambda^3/\Sigma\lambda^2$), to suppress the importance of smaller depressions, so that only "well-formed scallops" (Palmer, 2007, p.149) are included. Curl (1974: Equations 9 and 8) showed that:

$R_e' = 2200[2.5(\ln(w/2\lambda) - 1.0) + 9.4]$ (fissures) or
$R_e' = 2200[2.5(\ln(r/\lambda) - 1.5) + 9.4]$ (tubes)

Because the conduit flow Reynolds Number $R_e = \rho V(w \text{ or } 2r)/\mu = R_e'(w \text{ or } 2r)/\lambda$

$$R_e = (2200w/\lambda)[2.5(\ln(w/2\lambda) - 1.0) + 9.4] \text{ or} \quad \textbf{[5]}$$
$$R_e = (4400r/\lambda)[2.5(\ln(r/\lambda) - 1.5) + 9.4] \quad \textbf{[5]}$$

From $\lambda V = \mu R_e'/\rho$, these treatments show that the product λV differs for straight regular fissures or tubes:

$$\lambda V = (2200\mu/\rho)[2.5(\ln(w/2\lambda) - 1.0) + 9.4] \text{ or} \quad \textbf{[6]}$$
$$\lambda V = (2200\mu/\rho)[2.5(\ln(r/\lambda) - 1.5) + 9.4] \quad \textbf{[6]}$$

Curl (1966: p.153) deduced that stable scallops only form if their lengths are not greater than the conduit size, i.e. if $\lambda \leq (w \text{ or } 2r)$. He therefore identified a region of transitional turbulence where scallops do not form. However, the Curl (1974) treatment is based on the flow velocity at λ cm above the scallops, which, if $\lambda = (w \text{ or } 2r)$, would be at the opposite wall. It is therefore assumed here that scallops can only just start to form if $\lambda \leq (w/2 \text{ or } r)$ and that this occurs at R_{eF} at the onset of full turbulence in karst conduits. V_λ is then the *maximum* local flow velocity, in the centre of the conduit; (w/2 or r) represents the maximum possible scallop length for those conduit sizes at a mean conduit flow velocity of V_F. Substituting $\lambda = (w/2 \text{ or } r)$ in **[5]**, so that $\ln((w/2\lambda) \text{ or } r/\lambda) = 0$ and $\lambda_F V_F = \mu R_{eF}/2\rho$, for these initial scallop-forming conditions for fissures or tubes:

R_{eF} = 4400(6.9 or 5.65)
= (30,360 or 24,860) at any temperature
$\lambda_F V_F$ = (272 or 223) cm^2s^{-1} at 0°C
$\lambda_F V_F$ = (198 or 162) cm^2s^{-1} at 10°C

Because $\lambda V_\lambda = \mu R_{e\lambda}/\rho$, $V_F = (R_{eF}/2R_{e\lambda})V_\lambda = (0.723 \text{ or } 0.592)V_\lambda$ for fissures or tubes at the onset of full turbulence. From the Reynolds equation, scallops can form if $V \geq V_F \geq R_{eF}\mu/(w_F \text{ or } 2r_F)\rho$. From the D-W equation, $V^2 \geq (R_{eF}\mu/(w_F \text{ or } 2r_F)\rho)^2 \geq 4(w_F \text{ or } r_F)gi/f$. Thus, the minimum conduit sizes, hydraulic gradients and volumetric flow rates at which scallops can form are related by:

$(w_F \text{ or } r_F) = (2 \text{ or } 1)\lambda_F = ((R_{eF}^2\mu^2 f/(4 \text{ or } 16)\rho^2 gi))^{1/3}$
$i = V_F^2 f/4g(w_F \text{ or } r_F) = R_{eF}^2\mu^2 f/(4w_F^3 \text{ or } 16r_F^3)\rho^2 g$
$Q_F = (bw_F \text{ or } \pi r_F^2)V_F = (b \text{ or } \pi r_F/2)R_{eF}\mu/\rho$

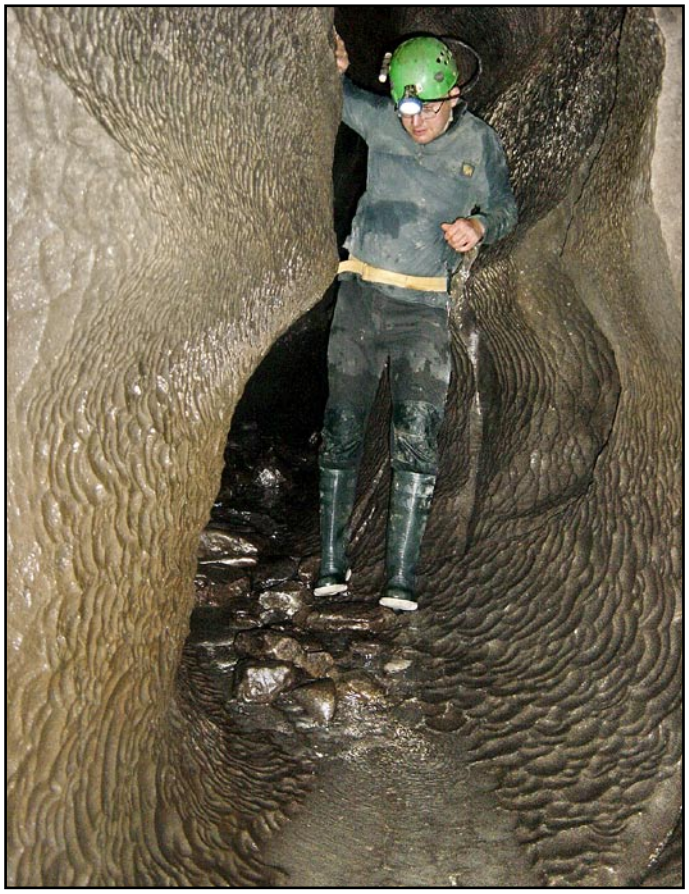

Figure 3: *Small-scale scallops and flutes in Poll Dubh, County Clare, Ireland.*

showing that the minimum conduit sizes for scallop formation vary with temperature, cross-section shape and the inverse of the cube root of hydraulic gradient. If f does not change during the enlargement of the conduit under constant head conditions from $f_T = (48 \text{ or } 64)/R_{eT}$ for fissures or tubes at the onset of transitional turbulence at $R_{eT} = 2200$ until full turbulence is reached, then, from the D-W and Reynolds equations:

$(w_F \text{ or } r_F) = ((48 \text{ or } 64)R_{eF}^2\mu^2/(4 \text{ or } 16)\rho^2 giR_{eT})^{1/3}$ and
Q_F = (544b or $700r_F^3$) cm^3s^{-1} at 0°C
Q_F = (397b or $510r_F^3$) cm^3s^{-1} at 10°C

The applicable flow rates for fissures or tubes are proportional to the breadth (but not the width) or the radius. However, the fissure calculations are less realistic at large sizes, when w≈b, so that a cylindrical tube may then be a better approximation.

Figure 4: *Scallops of length c. 7cm in Jengelgrotta, Norway, indicating a flow velocity of c. 55cm s^{-1}, assuming the scallop dominant discharge occurs during the spring melt.*

The required increases in conduit size after transitional turbulence therefore depend on $R_e^{2/3}$, giving:

$(w_F/w_T \text{ or } r_F/r_T) = (R_{eF}/R_{eT})^{2/3}$
$= ((30{,}360 \text{ or } 24{,}860)/2200))^{2/3}$
$= (13.8 \text{ or } 11.3)^{2/3} = 5.75 \text{ or } 5.04$
$(w_F \text{ or } r_F) = (1.181 \text{ or } 0.717)/i^{1/3}$ at 0°C **[7]**
$(w_F \text{ or } r_F) = (0.957 \text{ or } 0.581)/i^{1/3}$ at 10°C **[7]**

Thus, the size of any uniform fissure or tube needs to enlarge by a factor of (5.75 or 5.04) at any temperature from the onset of transitional turbulence to achieve full turbulence, at constant f and i. These relationships are also illustrated with logarithmic scales by the upper dashed lines on Figs 1 and 2. The slopes of these dashed lines also equal -0.333 log cm per log i, and so they are also parallel to the solid lines.

It is assumed that scallops cannot form at low hydraulic gradients until the conduit has enlarged so that scallops just appear in a large passage with $\lambda \leq (w/2 \text{ or } r)$. Therefore, if $\lambda = 200$cm is the largest observable scallop produced at the lowest velocity (Palmer, 2007), this occurs when $R_e = R_{eF}$ so that $V_F = \mu R_{eF}/(w \text{ or } 2r)\rho$ and:

$(w_F \text{ or } r_F) = (2 \text{ or } 1)\lambda_F = (400 \text{ or } 200)$ cm
$V_F = 1.361$ or 1.114 cm s^{-1} at 0°C
$V_F = 0.992$ or 0.812 cm s^{-1} at 10°C

These minimal mean velocities are close to the V = 1cm s^{-1} estimated by Palmer (2007). Because $V_\lambda = (2R_{e\lambda}/R_{eF})V_F = (2R_{e\lambda}/R_{eF})\mu R_{eF}/(w \text{ or } 2r)\rho = 2R_{e\lambda}\mu/400\rho$ in this case, then $V_\lambda = (1.88 \text{ and } 1.37)$ cm s^{-1} at 0°C and 10°C at the centres of these fissures or tubes. The largest possible observable scallops occur at only one particular hydraulic gradient and volumetric flow rate. If $f_T = (0.0218 \text{ or } 0.0291)$, these are, from **[7]**:

i $= (2.57 \text{ or } 4.60)10^{-8}$ at 0°C
i $= (1.37 \text{ or } 2.45)10^{-8}$ at 10°C
Q $= (0.544\text{b or } 140)$ litres s^{-1} at 0°C
Q $= (0.397\text{b or } 102)$ litres s^{-1} at 10°C

At higher friction factors, i increases in proportion to f. Conduits with steeper hydraulic gradients and faster flow rates and velocities will reach full turbulence at λ and $(w/2 \text{ or } r) < 200$cm. They can always eventually form shorter scallops under hydraulic control that may be more-easily observable if mechanical erosion does not dominate. Less-steep conduits can only form observable scallops after reaching full turbulence, when later enlarged to larger sizes with higher velocities, when $(w \text{ or } 2r) > 400$cm and $\lambda < 200$cm.

Possible coincidence of full turbulence and chemical breakthrough

During the enlargement of conduits of any length after transitional turbulence is reached at R_{eT}, calculations should be based on the D-W equation, even if breakthrough has not yet occurred. It is strictly incorrect to use the H-P equation here, despite the problem that modelling chemical breakthrough has only been reported for laminar flow so far. Nevertheless, if the flow is regarded as being more laminar than turbulent until the onset of full turbulence at R_{eF}, then, using w'_F or r'_F as the sizes for fissures or tubes for full turbulence for this assumption, from **[1]**:

$(w'_F \text{ or } r'_F) = ((12 \text{ or } 4)R_{eF}\mu^2/\rho^2 gi)^{1/3}$

The required increases in conduit size would then depend on $R_e^{1/3}$ (instead of $R_e^{2/3}$, as calculated above), giving, from **[2]**:

$(w'_F/w_T \text{ or } r'_F/r_T) = (R_{eF}/R_{eT})^{1/3}$
$= (13.8 \text{ or } 11.3)^{1/3} = 2.40 \text{ or } 2.24$
$(w'_F \text{ or } r'_F) = (0.492 \text{ or } 0.319)/i^{1/3}$ at 0°C
$(w'_F \text{ or } r'_F) = (0.399 \text{ or } 0.259)/i^{1/3}$ at 10°C

This is the basis on which breakthrough apertures for L = 1000m and 10,000m in Figures 1 and 2 have been constructed, for convenience, where the onset of full turbulence at $R_{eF} = (30{,}360 \text{ or } 24{,}860)$ for fissures or tubes is shown incorrectly by the middle dashed lines. The unlikely friction factors at the onset of full turbulence would then be $f = 48/R_{eF} = 0.00158$ or $f = 64/R_{eF} = 0.00257$.

A necessary condition for generating scallops is that the flowing water is sufficiently aggressive to dissolve the limestone. Whether possible scallop formation at full turbulence or chemical breakthrough occurs first during fissure or tube enlargement by dissolution can be considered from the ratios $(w_F/w_B \text{ or } r_F/r_B)$. These simplify to:

$w_F/w_B = (1.181/i^{1/3})/(0.0280/(i/L)^{1/3}) = 42.2/L^{1/3}$ at 0°C
$r_F/r_B = (0.717/i^{1/3})/(0.0167/(i/L)^{1/3}) = 42.9/L^{1/3}$ at 0°C
$w_F/w_B = (0.957/i^{1/3})/(0.0252/(i/L)^{1/3}) = 38.0/L^{1/3}$ at 10°C
$r_F/r_B = (0.581/i^{1/3})/(0.0150/(i/L)^{1/3}) = 38.6/L^{1/3}$ at 10°C

These ratios depend on temperature and the inverse of the cube root of the conduit length, but are similar (without being identical) for each conduit shape. The onsets of fully turbulent flow with possible scallop formation and first-order kinetics coincide at the same fissure or tube sizes if the ratios equal unity, giving:

L = (75,100 or 79,100) m at 0°C
L = (54,800 or 57,700) m at 10°C

for any hydraulic gradient and its related conduit size.

There are three length cases to be discussed, because transitional and possibly full turbulence may occur before or after breakthrough. In all cases under hydraulic control, once breakthrough is achieved, the conduit would then continue to enlarge at the S_{max} rate without limit. For conduits shorter than the previous coincidental lengths of 288–620m, the above ratios are >1 and chemical breakthrough occurs first in laminar flow. After transitional turbulence is reached, the conduit size has to increase by another factor of (5.75 or 5.04) to achieve full turbulence. At a low i of 10^{-5}, a 1m-long tube that needs a radius of 27cm to carry fully turbulent flow (Table 1) would only take another 220 years at S_{max} = 1mm a^{-1}. For L = 100m at i = 10^{-7}, the required radius increase from 15cm to 125cm would take 1100 years. At larger hydraulic gradients, all the timescales from breakthrough to full turbulence are reduced.

For conduit lengths between the previous coincident lengths and c. 55–80km, the ratios are >1 also, so that breakthrough could possibly occur before full turbulence. However, transitional turbulence increases the necessary conduit size and could delay breakthrough, as discussed before. The delay for conduits <10,000m long at i > 10^{-5}, or <1000m long at i > 10^{-7}, would not be significant *if the flow could be treated as almost laminar as R_e increases from R_{eT} to R_{eB}*. In these examples, conduits need only a half width or radius increase <10cm for breakthrough (Table 1), which could take <100 years if the dissolution rate approaches S_{max}. However, this may not be realistic, and for longer conduits and/or at lower values of i, the delays become more significant. If the flow is treated as turbulent immediately after laminar flow is lost, the dissolution rate S may remain well below S_{max}, so that delays are likely to be amplified and breakthrough might not occur, or only eventually at large conduit sizes. Taking a simplistic approach, if L = 10,000m at the low i of 10^{-9}, then a radius increase >200cm is needed for breakthrough. Even at the unrealistic post-breakthrough S_{max} rate of 1mm a^{-1}, this would take >2000 years. Hence, the delays to breakthrough in long conduits at low i may be significant. Thus, whether conduits are shorter or longer than the coincident lengths could be important for speleogenesis, especially as the coincidental lengths of 288–620m are based on the highest possible value of $R_{eT} = 2200$. Dissolution with high-order kinetics might create large conduits in long geological timescales, but breakthrough might never occur, depending on the conduit size at inception. A complication in natural systems is that it is rare for single, non-branching, conduits to be longer than 2km, without being joined by tributary conduits (Palmer, pers. comm.). These would modify downstream flow rates and provide opportunities for mixing corrosion to reduce breakthrough time. For conduits longer than c. 55–80km, full turbulence at $R_{eF} = (30{,}360 \text{ or } 24{,}860)$ would always start before chemical breakthrough at $R_{eB} > R_{eF}$, delaying it still further. However, such long conduits are not known in epigenic karst systems with meteoric recharge.

Any observable scallop in the wall of a phreatic passage with L < 10km at i > 10^{-5}, or <1km at i > 10^{-7} (and therefore in most known epigenic karst passages) probably formed when flow was fully turbulent and dissolution was at a maximum rate. This refines the conclusion reached by Faulkner (2004, p.44) who deduced that the applicable length is L < 5km, from the implicit assumption that scallops could form soon after the onset of transitional turbulence. However, the possibility that slow high-order dissolution kinetics might create wall scallops when acting in fully turbulent flow for enough time also needs to be considered. Conduits longer than 55km could occur in hypogenic systems, but these are characterized by the absence of wall scallops comparable to those in epigenic caves (Klimchouk, 2007, p.30).

This suggests that flows in purely hypogenic limestone aquifers never become fully turbulent, and from their commonly confined aquifers, probably do not even reach transitional turbulence or the chemical breakthrough point.

The demise of scallops at the onset of dominant mechanical erosion

Scallops reduce in length as V and R_e increase while the conduit enlarges by dissolution under hydraulic control, until mechanical erosion dominates. From **[6]** and the re-arranged D-W equation (w or r) = $V^2f/4gi$, if $\lambda_F = (w_F/2$ or $r_F)$ is the initial maximum scallop length when full turbulence is reached, $\ln(w_F/2\lambda_F$ or $r_F/\lambda_F) = 0$. If f and i remain constant, later relationships for fissures or tubes are given by:

$w/w_F = V^2/V_F^2 = (\lambda_F^2/\lambda^2)[(2.5\ln(w/2\lambda) + 6.9)/6.9]^2$

$w = (w_F^3/4\lambda^2)[(2.5\ln(w/2\lambda) + 6.9)/6.9]^2$ **[8]**

$r/r_F = V^2/V_F^2 = (\lambda_F^2/\lambda^2)[(2.5\ln(r/\lambda) + 5.65)/5.65]^2$

$r = (r_F^3/\lambda^2)[(2.5\ln(r/\lambda) + 5.65)/5.65]^2$ **[8]**

It is only when conduit sizes increase and scallops lengths decrease at any hydraulic gradient until w = 7.57λ (fissures) or r = 6.24λ (tubes) that the originally calculated values of λV = (403 and 294) cm^2s^{-1} apply at 0°C and 10°C. At these sizes, $R_e = wR_e'/\lambda = 7.57x22{,}500 = 170{,}000$ (fissures) or $R_e = 2rR_e'/\lambda = 2x6.24x22{,}500 = 281{,}000$ (tubes). If the smallest scallop that can exist before being removed by dominant mechanical erosion has λ_M = 1cm, then V_λ = (377 and 274) cm^2s^{-1} at 0°C and 10°C, roughly equal to the velocity $V_M = 300cm\ s^{-1}$, suggested by Palmer (2007). The conduit sizes (w_M or r_M) at which small scallops disappear at λ_M = 1cm are given, from **[8]**, by:

$w_M = (w_F^3/4)[(2.5\ln(w_M/2) + 6.9)/6.9]^2$

$w_M = (1.181^3/4i)[(2.5\ln(w_M/2) + 6.9)/6.9]^2$ at 0°C

$= (0.412/i)[(2.5\ln(w_M/2) + 6.9)/6.9]^2$

$w_M = (0.957^3/4i)[(2.5\ln(w_M/2) + 6.9)/6.9]^2$ at 10°C

$= (0.219/i)[(2.5\ln(w_M/2) + 6.9)/6.9]^2$

$r_M = r_F^3[(2.5\ln(r_M) + 5.65)/5.65]^2$

$r_M = (0.717^3/i)[(2.5\ln(r_M) + 5.65)/5.65]^2$ at 0°C

$= (0.369/i)[(2.5\ln(r_M) + 5.65)/5.65]^2$

$r_M = (0.581^3/i)[(2.5\ln(r_M) + 5.65)/5.65]^2$ at 10°C

$= (0.196/i)[(2.5\ln(r_M) + 5.65)/5.65]^2$

Thus, the minimum conduit sizes for the onsets of dominant mechanical erosion vary both with temperature and with cross-section shape, but not at a standard Reynolds Number and they have a complex relationship with (w_F or r_F) and i. These equations are valid only for ($w_M/2$ or r_M) ≥ 1cm, which are the smallest sizes at which scallops can appear (see below). From **[6]**, the following values would apply for a large conduit with (w/2 or r) = 5m and with 1cm-long scallops that are about to be removed by mechanical erosion:

$\lambda_M V_M = V_M = (2200\mu/\rho)[2.5\ln500 + 6.9]$ or

$\lambda_M V_M = V_M = (2200\mu/\rho)[2.5\ln500 + 5.65]$

$\lambda_M V_M = V_M =$ (885 or 835) cm^2s^{-1} or $cm\ s^{-1}$ at 0°C

$\lambda_M V_M = V_M =$ (645 or 609) cm^2s^{-1} or $cm\ s^{-1}$ at 10°C

i = (0.0044 or 0.0104) at 0°C

i = (0.0023 or 0.0055) at 10°C

Q_M = (0.885b or 656) m^3s^{-1} at 0°C

Q_M = (0.645b or 478) m^3s^{-1} at 10°C

R_{eM} = (4.94 or 4.66)10^7 at both 0°C and 10°C

Here, $V_M = (2.35$ or $2.22)V_\lambda$ (fissures or tubes) at all temperatures. Although for tubes at 10°C, V varies from 162 to 609$cm\ s^{-1}$ and V/V_λ varies from $V_F/V_\lambda = 0.592$ to $V_M/V_\lambda = 2.22$, these values are relatively insensitive to conduit radii in the 500-fold range from 1cm to 5m. However, λV_λ = (377 and 274) $cm^2\ s^{-1}$ at 0°C and 10°C should remain constant for all conduits that generate scallops from λ = 200cm until mechanical erosion dominates at λ = 1cm. This includes cases where these extreme and intermediate sizes occur at the onset of full turbulence. The above conduit represents extreme, but possible, conditions for peak flow rate. It would have initially have gained transitional turbulence at (w_T or r_T) = (1.3 or 0.65)cm and started to form scallops at the onset of full turbulence when (w_F or r_F) = (7.2 or 3.3)cm and λ = (3.6 or 3.3)cm. These values are fairly close to the minimum size for the formation of scallops. For conduits with decreasing hydraulic gradients, the sizes for dominant mechanical erosion increase, and the required flow rate increases dramatically. It follows that the mechanical erosion of scallops is a rare occurrence that requires relatively steep conduits and large flow rates from large catchment areas. It also only applies to scallops that were already short when formed in tiny conduits.

Possible coincidences with dominant mechanical erosion

The possibility that the onset of dominant mechanical erosion might coincide with the onset of full turbulence can be considered by calculating the ratio of required conduit sizes, as derived above. Because scallop size λ_M = 1cm at the erosion onset, and $\lambda_F = (w_F/2$ or $r_F)$ at the start of full turbulence, this coincidence can only occur at a conduit size of w = 2cm or r = 1cm. Such scallops could only exist fleetingly, at one particular hydraulic gradient at which the flow velocity reaches the value of V_F that allows scallops to form at the onset of full turbulence, just as the velocity becomes high enough at V_M for mechanical erosion to prevent scallops. It is assumed here that this occurs if $V_M = V_F$ and $R_{eM} = R_{eF}$ at $\lambda_M = \lambda_F$ = 1cm for a tiny conduit that cannot be observed directly, with $w_M = w_F$ = 2cm or $r_M = r_F$ = 1cm. Then, $\ln(w_F/2\lambda_F$ or $r_F/\lambda_F) = 0$ and the terms within square parentheses simplify to unity. Thus, for this coincidence, from **[8]** and **[7]**:

$w_M/w_F = (w_F^3/4\lambda_M^2w_F)[(2.5\ln(w_M/2\lambda_M) + 6.9)/6.9]^2 = w_F^2/4$

$= ((1.181^2$ and $0.957^2)/4i^{2/3})$ at 0°C and 10°C

$= ((0.349$ and $0.229)/i^{2/3})$ at 0°C and 10°C

$r_M/r_F = (r_F^3/\lambda_M^2r_F)[(2.5\ln(r_M/\lambda_M) + 5.65)/5.65]^2 = r_F^2$

$= ((0.717^2$ and $0.581^2)/i^{2/3})$ at 0°C and 10°C

$= ((0.514$ and $0.337)/i^{2/3})$ at 0°C and 10°C

For unity

i = (0.206 and 0.110) at 0°C and 10°C for fissures or

i = (0.369 and 0.196) at 0°C and 10°C for tubes

$V_M = V_F = \lambda_F V_F/\lambda_F$ = (272 or 223) $cm\ s^{-1}$ at 0°C and

V_M = (198 or 162) $cm\ s^{-1}$ at 10°C

V_λ = (377 and 274) $cm\ s^{-1}$ at 0°C and 10°C for both fissures or tubes

Q = (544b or 700) cm^3s^{-1} at 0°C for fissures or tubes

Q = (397b or 510) cm^3s^{-1} at 10°C for fissures or tubes

Thus, the dominant mechanical erosion flow velocity could apply before the onset of full turbulence only in steep fissures or tubes with the applicable hydraulic gradient larger than the range 0.1–0.4. Conduits with a smaller i would reach V_M and λ_M after full turbulence is reached, at larger conduit sizes that may be enterable. Such conduits may have observable scallops with λ > 1cm, if dominant mechanical erosion did not occur later. Conduits along steeper hydraulic gradients, including all those situated beneath reservoirs or lakes with lower outlets with i > 1, would never form scallops whilst under constant head conditions. Their flows could change from laminar or transitional turbulence directly to the c. 300$cm\ s^{-1}$ speed otherwise required for scallop demise, at conduit sizes (w/2 or r) < 1cm. These conditions can occur naturally during sudden creation of karstic short cuts below reservoir dams and during jökulhlaups, if ice-dammed lakes collapse to a lower level via a karst conduit. However, the behaviour of flows in such steep small conduits is unclear. Despite the velocity exceeding V_M, mechanical erosion by sediment load alone may be restricted because the flow would be incapable of creating and/or transporting large grains of bedrock.

Comparing dominant mechanical erosion with the onset of first-order kinetics, from **[8]**, **[7]** and **[4]**:

$w_M/w_B = (w_F^3/4\lambda_M^2w_B)[(2.5\ln(w_M/2\lambda_M) + 6.9)/6.9]^2$

$= ((1.181^3/4i)/(0.0280/(i/L)^{1/3})$ and

$(0.957^3/4i)/(0.0252/(i/L)^{1/3}))[(2.5\ln(w_M/2) + 6.9)/6.9]^2$

at 0°C and 10°C

$= (14.7$ and $8.69)[(2.5\ln(w_M/2) + 6.9)/6.9]^2/(i^{2/3}L^{1/3})$

at 0°C and 10°C

$r_M/r_B = (r_F^3/\lambda_M^2r_B)[(2.5\ln(r_M/\lambda_M) + 5.65)/5.65]^2$

$= ((0.717^3/i)/(0.0167/(i/L)^{1/3})$ and

$(0.581^3/i)/(0.0150/(i/L)^{1/3}))[(2.5\ln(r_M)+5.65)/5.65]^2$

at 0°C and 10°C

$= (22.1$ and $13.0)[(2.5\ln(r_M) + 5.65)/5.65]^2/(i^{2/3}L^{1/3})$

at 0°C and 10°C

For unity:

$L = (3190 \text{ and } 657)[(2.5\ln(w_M/2) + 6.9)/6.9]^6/i^2$ at 0°C and 10°C for fissures

$L = (10{,}700 \text{ and } 2210)[(2.5\ln(r_M) + 5.65)/5.65]^6)/i^2$ at 0°C and 10°C for tubes.

These equations can easily be solved for the triple coincidence of full turbulence, dominant mechanical erosion and first-order kinetics that might arise when (w/2 or r) = 1cm. The terms within square parentheses then simplify to unity. Substituting the unique values of i above for the coincidence of dominant mechanical erosion with full turbulence:

$L = (3190/0.206^2 \text{ and } 657/0.110^2)$ at 0°C and 10°C for fissures

L = (75,100 and 54,800) at 0°C and 10°C for fissures

or

$L = (10{,}700/0.369^2 \text{ and } 2210/0.196^2)$ at 0°C and 10°C for tubes

L = (79,100 and 57,700) at 0°C and 10°C for tubes

Hence, for this particular case, these long and unrealistic lengths are the same as calculated previously for coincidence of full turbulence and breakthrough at any hydraulic gradient and its related conduit size. Coupled with the large heads required, it follows that for all shorter karst conduits (i.e. for all natural conduits) with this particular or any lower hydraulic gradient, chemical breakthrough always occurs before dominant mechanical erosion. Also, at the rather high hydraulic gradient of i > 0.1, the delay to breakthrough in long conduits caused by transient turbulence should be insignificant.

The previous analysis is inappropriate for hydraulic gradients larger than the range 0.1–0.4 and before conduit size reaches (w/2 or r) = 1cm, but the D-W equation can be used to determine the hydraulic gradient required for the mean flow velocity to reach c. 300cm s^{-1} at any size. This can then be used to determine the longest length of conduit of that size that can maintain first-order dissolution kinetics before that speed is reached, whilst also considering the practicality of the large heads required at high values of i. The deepest reservoirs can provide H ≤ 40m, ice-dammed lakes in Central Scandinavia reached depths up to c. 500m during Weichselian deglaciation (Faulkner, 2005), and Lake Baikal is the deepest natural lake at c. 1600m depth. If the shortest karst fissure below a reservoir dam is 8m long, i ≤ 5, but all fissures shorter than 228m would achieve chemical breakthrough at w = 0.1cm before V = 300cm s^{-1}. Longer fissures would reduce i and V, so that this priority is true for all reservoirs. However, any karst fissures with L ≤ 50m to valley outlets below the bottom of 500m-deep ice-dammed lakes would have i > 10, which is close to the point of coincidence. Thus, it is just feasible (but unlikely) that such deglacial flows at 0°C could reach the velocity of dominant mechanical erosion first. Any karst conduits draining 1600m-deep natural lakes would need to be shorter than c. 320m with i = 5 for this condition, but no such systems are known. In conclusion, therefore, it is unlikely that any karst conduits would experience dominant mechanical erosion before reaching the chemical breakthrough point.

Recharge conditions, flow regimes and conduit geometry

In practical karst systems there are three basic recharge conditions, seven basic flow regimes, and two basic long profile conduit geometries to consider, when discussing the chemical and mechanical evolution of conduits. Other important speleogenetic processes, including clastic sedimentation, cavern breakdown and condensation corrosion, are beyond the scope of this paper. The basic recharge conditions are:

1 Constant head condition (hydraulic control), which provides increasing recharge. H, i, L and i/L stay constant and the flow remains wholly phreatic as Q, V and R_e continually increase as the conduit size increases by dissolution. This applies whilst the conduit entrance remains flooded by a stream, lake or reservoir.

2 Constant recharge condition (catchment control), where Q remains constant but H, i and V reduce as the conduit size increases. This applies to many mature karst systems fed by allogenic recharge, when averaged over several years. Q may only equal the maximum recharge reached under a previous hydraulic control regime if the source is a stream or river. If a source lake dries up or a reservoir collapses, the new flow rate will be reduced.

3 Reducing recharge condition, where Q reduces into the conduit, causing a direct reduction in H, i, V and R_e. This applies either continuously or suddenly, if some of the allogenic underground recharge is captured upstream, or if the recharge reduces under climatic control, or if uplift and/or tectonic movements and/or surface erosion cause changes to the local topography and hydrology.

The first four flow regimes have already been introduced, and the other three are discussed below. They are all simply listed as:

a. Phreatic laminar;
b. Phreatic transitionally turbulent;
c. Phreatic fully turbulent, with the possible formation of scallops;
d. Phreatic dominant mechanical erosion, with the removal or prevention of scallops;
e. Vadose. Although vadose flows could theoretically replicate the phreatic regimes, it is assumed herein that only turbulent flows are important and that chemical vadose entrenchment is commonly at the S_{max} rate;
f. Static, when there is no recharge into, or discharge from, a phreatic loop or a pool in an open conduit;
g. Relict, when there is no flowing or static water in the conduit.

The basic long profiles are for conduits from an upper sink to a lower resurgence that:

x. Continuously descend, without any rising parts;
y. Reach below the elevation of the resurgence, to form a single descending then rising phreatic loop.

Conduit evolution for long profiles with multiple phreatic loops above and/or below resurgence level is more complex, but could be analysed by considering each loop separately.

Visualization of conduit evolution in phreatic conditions

Most previous analyses of the evolution of a single conduit have concentrated on constant head conditions, with little attention being paid to other recharge conditions, the flow regimes, and their possible dependence on the long profile of the initial hydraulic system. The following discussions briefly consider the variations in fissure or tube evolution during each flow regime before and after chemical breakthrough for each type of profile, under each condition of recharge. These are summarized in Table 2 and can be visualized on Figure 1 or 2. The log i x-axis values are chosen to exceed the extreme ranges likely to apply in natural and artificial karst systems. However, the conduit size can increase beyond the 10m width or radius on the y-axis. Thus, values go beyond the 'central' ranges of i from 10^{-4} to 10^{-2}, conduit sizes from 1mm to 10cm, conduit lengths from 100–1000m, and R_e = 2200. Each main combination is labelled 1x, 1y, 2x, 2y, 3x and 3y. For all these cases, the coincidental lengths remain the same as calculated previously, provided they only represent the phreatic part of the conduit at the two transitions.

Constant head conditions

Whilst constant head conditions can be maintained, conduit evolution is independent of its long profile type, i.e. combinations 1x and 1y can be treated as discussed in previous sections for the first four flow regimes. The continuing hydrogeological evolution of conduit size for one of the plotted lengths can be visualized on Figure 1 or 2 by moving vertically up the graph at a constant i on the x-axis from an assumed initial conduit size on the y-axis. For small conduits with L up to the coincidental lengths (which would coincide with the lowest dashed lines), enlargement starts slowly with high-order kinetics in laminar flow, but at an increasing rate until the applicable solid line for the conduit length is reached at the breakthrough point. This point indicates the required conduit size on the y-axis. It is shown correctly by the solid lines for L = 1m, 10m and 100m at R_{eB} = 7.65, 76.5 and 765 (fissures) or at R_{eB} = 4.87, 48.7 and 487 (tubes). Dissolution then proceeds at the S_{max} rate in laminar flow and continues at that rate when transitional turbulent flow is reached at R_e = 2200 and fully turbulent flow at R_e = (30,360 or 24,860) for fissures or tubes, at the lowest and highest dashed lines. (The highest dashed lines represent R_{eF} assuming that the D-W equation applies during transitional turbulence). Thereafter, scallops may form until dominant mechanical erosion is reached (not shown).

Conduit shape	Recharge	Onset parameter	Temperature	Conduit length L = shorter than coincidental length				Conduit length L = longer than coincidental length			
				Flow regime				Flow regime			
				Laminar	Transitional turbulence	Full turbulence	Dominant mechanical erosion	Laminar	Transitional turbulence	Full turbulence	Dominant mechanical erosion
				Flow equation				Flow equation			
				H-P	D-W	D-W	D-W	H-P	D-W	D-W	D-W
Fissure	Constant head	Flow regime		Flow regime advances from laminar towards dominant mechanical erosion whilst constant head is maintained as the fissure enlarges							
			0°C	$w < w_T$ $R_e < R_{eT}$	$w_T = 0.2053/i^{1/3}$ $R_{eT} = 2200$	$w_F = 1.1814/i^{1/3}$ $R_{eF} = 30,360$	$w_M = 0.4122[\ ]^{2/i}$ $\lambda = 1cm$	$w < w_T$ $R_e < R_{eT}$	$w_T = 0.2053/i^{1/3}$ $R_{eT} = 2200$	$w_F = 1.1814/i^{1/3}$ $R_{eF} = 30,360$	$w_M = 0.4122[\ ]^{2/i}$ $\lambda = 1cm$
			10°C	$w < w_T$ $R_e < R_{eT}$	$w_T = 0.1663/i^{1/3}$ $R_{eT} = 2200$	$w_F = 0.9569/i^{1/3}$ $R_{eF} = 30,360$	$w_M = 0.2190[\ ]^{2/i}$ $\lambda = 1cm$	$w < w_T$ $R_e < R_{eT}$	$w_T = 0.1663/i^{1/3}$ $R_{eT} = 2200$	$w_F = 0.9569/i^{1/3}$ $R_{eF} = 30,360$	$w_M = 0.2190[\ ]^{2/i}$ $\lambda = 1cm$
		Chemical regime		Chemical kinetics advance to post-breakthrough first-order reaction rate				Breakthrough may be achieved, dependent on length and i			
			0°C	$w_B = 0.0280/(i/L)^{1/3}$ $R_{eB} = 5.5772L$	First-order reaction kinetics Reaction rate = S_{max}			High-order kinetics Reaction rate << S_{max}	S_{max}: $w_B > 0.0280/(i/L)^{1/3}$ $R_{eB} > 5.5772L$		S_{max}
			10°C	$w_B = 0.0252/(i/L)^{1/3}$ $R_{eB} = 7.6511L$					S_{max}: $w_B > 0.0252/(i/L)^{1/3}$ $R_{eB} > 7.6511L$		
	Constant recharge	Flow regime	0°C	Flow regime remains locked into its new state at the initiation of constant recharge at a constant R_e as the fissure enlarges, whilst w << b							
			10°C								
		Chemical regime	0°C	Chemical kinetic order remains locked into its new pre- or post-breakthrough state during constant recharge at a constant R_e as the fissure enlarges, whilst w << b							
			10°C								
	Reducing discharge	Flow regime		Flow regime retreats from dominant mechanical erosion towards laminar during reducing recharge as the fissure enlarges							
			0°C	$w < w_T$ $R_e < R_{eT}$	$w_T = 0.2053/i^{1/3}$ $R_{eT} = 2200$	$w_F = 1.1814/i^{1/3}$ $R_{eF} = 30,360$	$w_M = 0.4122[\ ]^{2/i}$ $\lambda = 1cm$	$w < w_T$ $R_e < R_{eT}$	$w_T = 0.2053/i^{1/3}$ $R_{eT} = 2200$	$w_F = 1.1814/i^{1/3}$ $R_{eF} = 30,360$	$w_M = 0.4122[\ ]^{2/i}$ $\lambda = 1cm$
			10°C	$w < w_T$ $R_e < R_{eT}$	$w_T = 0.1663/i^{1/3}$ $R_{eT} = 2200$	$w_F = 0.9569/i^{1/3}$ $R_{eF} = 30,360$	$w_M = 0.2190[\ ]^{2/i}$ $\lambda = 1cm$	$w < w_T$ $R_e < R_{eT}$	$w_T = 0.1663/i^{1/3}$ $R_{eT} = 2200$	$w_F = 0.9569/i^{1/3}$ $R_{eF} = 30,360$	$w_M = 0.2190[\ ]^{2/i}$ $\lambda = 1cm$
		Chemical regime		Kinetics retreat via limiting recharge point to high-order reaction rate				Retreat back to high-order kinetics if breakthrough previously achieved			
			0°C	$w_B = 0.0280/(i/L)^{1/3}$ $R_{eB} = 5.5772L$	First-order reaction kinetics Reaction rate = S_{max}			High-order kinetics Reaction rate << S_{max}	S_{max}: $w_B > 0.0280/(i/L)^{1/3}$ $R_{eB} > 5.5772L$		S_{max}
			10°C	$w_B = 0.0252/(i/L)^{1/3}$ $R_{eB} = 7.6511L$					S_{max}: $w_B > 0.0252/(i/L)^{1/3}$ $R_{eB} > 7.6511L$		
Tube	Constant head	Flow regime		Flow regime advances from laminar towards dominant mechanical erosion whilst constant head is maintained as the tube enlarges							
			0°C	$r < r_T$ $R_e < R_{eT}$	$r_T = 0.1424/i^{1/3}$ $R_{eT} = 2200$	$r_F = 0.7170/i^{1/3}$ $R_{eF} = 24,860$	$r_M = 0.3685[\ ]^{2/i}$ $\lambda = 1cm$	$r < r_T$ $R_e < R_{eT}$	$r_T = 0.1424/i^{1/3}$ $R_{eT} = 2200$	$r_F = 0.7170/i^{1/3}$ $R_{eF} = 24,860$	$r_M = 0.3685[\ ]^{2/i}$ $\lambda = 1cm$
			10°C	$r < r_T$ $R_e < R_{eT}$	$r_T = 0.1153/i^{1/3}$ $R_{eT} = 2200$	$r_F = 0.5807/i^{1/3}$ $R_{eF} = 24,860$	$r_M = 0.1958[\ ]^{2/i}$ $\lambda = 1cm$	$r < r_T$ $R_e < R_{eT}$	$r_T = 0.1153/i^{1/3}$ $R_{eT} = 2200$	$r_F = 0.5807/i^{1/3}$ $R_{eF} = 24,860$	$r_M = 0.1958[\ ]^{2/i}$ $\lambda = 1cm$
		Chemical regime		Chemical kinetics advance to post-breakthrough first-order reaction rate				Breakthrough may be achieved, dependent on length and i			
			0°C	$r_B = 0.0167/(i/L)^{1/3}$ $R_{eB} = 3.5506L$	First-order reaction kinetics Reaction rate = S_{max}			High-order kinetics Reaction rate << S_{max}	S_{max}: $r_B > 0.0167/(i/L)^{1/3}$ $R_{eB} > 3.5506L$		S_{max}
			10°C	$r_B = 0.0150/(i/L)^{1/3}$ $R_{eB} = 4.8708L$					S_{max}: $r_B > 0.0150/(i/L)^{1/3}$ $R_{eB} > 4.8708L$		
	Constant recharge	Flow regime		Flow regime retreats from possible dominant mechanical erosion towards laminar whilst constant recharge is maintained as the tube enlarges							
			0°C	$r < r_T$ $R_e < R_{eT}$	$r_T = 0.1424/i^{1/3}$ $R_{eT} = 2200$	$r_F = 0.7170/i^{1/3}$ $R_{eF} = 24,860$	$r_M = 0.3685[\ ]^{2/i}$ $\lambda = 1cm$	$r < r_T$ $R_e < R_{eT}$	$r_T = 0.1424/i^{1/3}$ $R_{eT} = 2200$	$r_F = 0.7170/i^{1/3}$ $R_{eF} = 24,860$	$r_M = 0.3685[\ ]^{2/i}$ $\lambda = 1cm$
			10°C	$r < r_T$ $R_e < R_{eT}$	$r_T = 0.1153/i^{1/3}$ $R_{eT} = 2200$	$r_F = 0.5807/i^{1/3}$ $R_{eF} = 24,860$	$r_M = 0.1958[\ ]^{2/i}$ $\lambda = 1cm$	$r < r_T$ $R_e < R_{eT}$	$r_T = 0.1153/i^{1/3}$ $R_{eT} = 2200$	$r_F = 0.5807/i^{1/3}$ $R_{eF} = 24,860$	$r_M = 0.1958[\ ]^{2/i}$ $\lambda = 1cm$
		Chemical regime		Kinetics retreat via limiting recharge point to high-order reaction rate				Retreat back to high-order kinetics if breakthrough previously achieved			
			0°C	$r_B = 0.0167/(i/L)^{1/3}$ $R_{eB} = 3.5506L$	First-order reaction kinetics Reaction rate = S_{max}			High-order kinetics Reaction rate << S_{max}	S_{max}: $r_B > 0.0167/(i/L)^{1/3}$ $R_{eB} > 3.5506L$		S_{max}
			10°C	$r_B = 0.0150/(i/L)^{1/3}$ $R_{eB} = 4.8708L$					S_{max}: $r_B > 0.0150/(i/L)^{1/3}$ $R_{eB} > 4.8708L$		
	Reducing discharge	Flow regime		Flow regime retreats from possible dominant mechanical erosion towards laminar during reducing recharge as the tube enlarges							
			0°C	$r < r_T$ $R_e < R_{eT}$	$r_T = 0.1424/i^{1/3}$ $R_{eT} = 2200$	$r_F = 0.7170/i^{1/3}$ $R_{eF} = 24,860$	$r_M = 0.3685[\ ]^{2/i}$ $\lambda = 1cm$	$r < r_T$ $R_e < R_{eT}$	$r_T = 0.1424/i^{1/3}$ $R_{eT} = 2200$	$r_F = 0.7170/i^{1/3}$ $R_{eF} = 24,860$	$r_M = 0.3685[\ ]^{2/i}$ $\lambda = 1cm$
			10°C	$r < r_T$ $R_e < R_{eT}$	$r_T = 0.1153/i^{1/3}$ $R_{eT} = 2200$	$r_F = 0.5807/i^{1/3}$ $R_{eF} = 24,860$	$r_M = 0.1958[\ ]^{2/i}$ $\lambda = 1cm$	$r < r_T$ $R_e < R_{eT}$	$r_T = 0.1153/i^{1/3}$ $R_{eT} = 2200$	$r_F = 0.5807/i^{1/3}$ $R_{eF} = 24,860$	$r_M = 0.1958[\ ]^{2/i}$ $\lambda = 1cm$
		Chemical regime		Faster kinetics retreat via limiting recharge point to high-order reaction rate				Faster retreat to high-order kinetics if breakthrough previously achieved			
			0°C	$r_B = 0.0167/(i/L)^{1/3}$ $R_{eB} = 3.5506L$	First-order reaction kinetics Reaction rate = S_{max}			High-order kinetics Reaction rate << S_{max}	S_{max}: $r_B > 0.0167/(i/L)^{1/3}$ $R_{eB} > 3.5506L$		S_{max}
			10°C	$r_B = 0.0150/(i/L)^{1/3}$ $R_{eB} = 4.8708L$					S_{max}: $r_B > 0.0150/(i/L)^{1/3}$ $R_{eB} > 4.8708L$		

Table 2: *Onsets of flow regimes and first-order reaction kinetics during phreatic conduit evolution*

For longer conduits, transitional turbulent flow is reached before breakthrough at the lowest dashed lines. This is therefore delayed by an uncertain amount of time, and occurs at an uncertain conduit size larger than shown by the solid lines for L = 1000m and 10,000m. These are drawn as though laminar flow still applies (as assumed by previous models) at R_e = 7650 and 76,500 (for fissures) or at R_e = 4870 and 48,700 (for tubes), as are the middle dashed line representations of R_{eF}. If and when breakthrough is reached, dissolution then proceeds at the S_{max} rate in transitional and then full turbulence, with possible scallop formation, until dominant mechanical erosion applies. For all conduits under constant head conditions, once turbulent flow and first-order kinetics are achieved, they will always be maintained, and conduit sizes will increase linearly with time by chemical dissolution. Growth also accelerates with increasing mechanical erosion, and vadose flow is never achieved.

Constant recharge conditions

For all downward-trending conduits 2x, when the size increases so that the flow capacity of the conduit exceeds the recharge available, the flow will become vadose along the whole length of the conduit (Palmer, 1991: 5–6). This will occur whenever the sink entrance is no longer completely submerged and can apply before or after breakthrough, during any flow regime. Dissolution is then under open vadose conditions with the CO_2 in the water equilibrating with the air along the conduit, which may have a higher or lower P_{CO2} than when under hydraulic control. The calcite saturation concentration is higher than in the closed phreatic case (Palmer, 1991), increasing the penetration length. The mathematics of chemical dissolution in vadose conditions awaits evaluation. However, chemical vadose entrenchment will occur at the S_{max} rate where the calcite concentration remains below 60–90% of saturation, dependent on temperature and P_{CO2}. The common presence of scallops on the walls of vadose stream passages indicates their formation in fully turbulent flow at high stage, most probably at the S_{max} rate.

For conduits that form single phreatic loops 2y, when their capacities exceed the recharge during any flow regime, the flow will become vadose from the sink entrance to a water surface that is slightly above the level of the resurgence. This will immediately reduce H, i and L for the continuing phreatic flow by amounts that depend on the long profile of the conduit. Thereafter, H and i will continue to reduce as the conduit size increases by dissolution. This would also cause L to continue to reduce slightly, but this effect should be negligible for long conduits. The immediate impact on the kinetic order depends on the geometry. The required w_B or r_B and T_B will all increase with reduced i if pre-breakthrough, whereas the reduced L would have the opposite effect. (Noting that less limestone needs to be dissolved along the conduit and without considering the chemical changes in the vadose part). Thus, the new chemical kinetics could initially remain unchanged or move either way between pre- and post-breakthrough, before embarking on the evolution discussed empirically below.

The evolution of the lower phreatic part of conduit 2y, after the establishment of constant recharge at any hydraulic gradient and at any conduit size, can be visualized in Figure 1 or 2 by moving from that point diagonally upwards to the left as i reduces whilst the size increases, either slowly if pre-breakthrough in laminar or turbulent flow, or at the S_{max} rate if post-breakthrough in laminar or turbulent flow. If the flow is laminar after the onset of constant recharge, from the H-P equation for fissures or tubes:

$i = 12\mu Q/\rho g b w^3$ or $i = 8\mu Q/\pi\rho g r^4$

so that, at constant recharge, i is inversely proportional to w^3 or r^4, and

$w = (12\mu Q/\rho g b i)^{1/3}$ or $r = (8\mu Q/\pi\rho g i)^{1/4}$

From Figure 1 or Figure 2, the slopes of the logarithms of these functions would be -0.333 (fissures) or -0.250 (tubes) log cm per log i. If the flow is turbulent, from the D-W equation for fissures or for tubes:

$i = fQ^2/4gb^2w^3$ or $i = fQ^2/4\pi^2gr^5$

so that, at constant recharge, i is inversely proportional to w^3 or r^5, and

$w = (fQ^2/4gb^2i)^{1/3}$ or $r = (fQ^2/4\pi^2gi)^{1/5}$

The slopes of the logarithms of these functions on Figure 1 or 2 would be -0.333 (for fissures) or -0.200 (for tubes) log cm per log i.

Thus, the effects on the flow regimes of planar fissures and cylindrical tubes differ after constant recharge Q is initiated and there is a need to consider all the various possibilities. For fissures, Q = bwV and $R_e = w\rho V/\mu = \rho Q/b\mu$. Therefore, the fissure flow regime remains 'locked' into its new state at a constant R_e, whilst the dissolutional increase in w is balanced by the reduction in V. (However, dominant mechanical erosion would cease when λ = 1cm). In fully turbulent flow, scallops will now lengthen from their size at the onset of constant recharge as V reduces. From the previous analysis, $\lambda/w = (377 \text{ and } 274)\rho V/\mu R_e V_\lambda$ at 0°C and 10°C and so is proportional to V/V_λ. This ratio slowly increases until scallops become unrecognizable when λ = 200cm, in a passage that is even wider. The R_e at which dissolution changes between high- and first-order kinetics is a constant for each L, because $R_{eB} = 0.1L\rho/\mu$. Therefore, the chemical kinetic order would also be locked into its new state during constant recharge, which would depend partly on whether L is less or more than the coincident length. Thus, the fissure would either continue to widen at the same slow rate if pre-breakthrough (with the penetration length remaining constant), and therefore never achieve breakthrough, or it would continue to enlarge indefinitely at the fast S_{max} rate if post-breakthrough. The -0.333 log cm per log i slope of log w for fissures in both laminar and turbulent flow under constant recharge is the same as for the existing lines on Figure 1. This also illustrates that both the flow and chemical regimes remain locked during conduit enlargement, which is therefore visualized by moving diagonally upwards at the same angle. There is initially no "limiting recharge point" for fissures under constant recharge conditions, as was assumed by Faulkner (2006a, 14–15). However, all conduits that start as fissures will become more square-shaped as the width increases, so that they will eventually behave more like a cylindrical tube, as discussed next.

For tubes, $Q = \pi r^2 V$ and $R_e = 2r\rho V/\mu = 2\rho Q/\pi r\mu$, and so R_e reduces as the radius r continues to expand, whilst V reduces with r^2. Hence, Q and V become insufficient to maintain the new flow and chemical regimes. The tube flow regime immediately starts to reverse back through its previous flow regimes, ultimately regaining laminar flow. The previous r_F and r_T relationships apply, with these reverse transitions also occurring when $R_e = R_{eF}$ = 24,860 and then when $R_e = R_{eT}$ = 2200, whilst assuming f = 0.0291, but at larger tube sizes than occurred under the earlier constant head conditions. Whilst under full turbulence, scallops will also lengthen, as they do for fissures. The ratio $\lambda/2r = (377 \text{ and } 274)\rho V/\mu R_e V_\lambda$ at 0°C and 10°C will increase faster than for fissures as R_e decreases. The scallops will cease to form when λ = r at $R_e = R_{eF}$ = 24,860, or become unrecognizable in a large cylindrical sump when λ ≥ 200cm. Presumably, scallops of any size existing when R_e < 24,860 will fade away by dissolution. The reaction kinetics would also weaken at the onset of constant recharge, as realized by Palmer (1981). If the tube flow is initially post-breakthrough, dissolution would continue at the S_{max} rate until slow high-order kinetics is regained at the limiting recharge point. This occurs when R_e reduces to $R_{eB} = 0.2L\rho/\pi\mu$ and the penetration length approaches the length of the phreatic part of the conduit. The penetration length would continue to shrink and further enlargement would eventually cease, or be significant only over long geological timescales or with mixing corrosion. The tube size at the limiting recharge point obeys the same r_B relationship as derived for chemical breakthrough, although the actual sizes will be larger than before. Whether the reverse flow regime transitions occur before or after the limiting recharge point under catchment control depends on the ratios previously calculated. Hence, they depend on whether L, the length of the phreatic part of the tube, is shorter or longer than the applicable coincidental length. For tubes equal to the same coincidental lengths as calculated for breakthrough and transitional turbulence, the tube size and time relationships calculated by Faulkner (2006a) apply. However, it was assumed implicitly therein that reversions to laminar flow and high-order kinetics would coincide. For tubes shorter than the coincidental lengths, faster laminar flow occurs before the onset of slower high-order kinetics, which is therefore delayed slightly. For tubes longer than the coincidental lengths, the onset of high-order kinetics occurs whilst the flow velocity is still slowed by turbulence and the new low dissolution rate is reduced further.

If the tube is in turbulent flow at the onset of constant recharge, the -0.200 log cm per log i slope of log r is less steep than the dashed lines on Figure 2. The new trend line will intersect the highest and/or lowest dashed lines at points that indicate the hydraulic gradient and radius at

the changes back to transitional turbulent then laminar flow. For tubes shorter than the coincidental lengths, the lowest dashed line will be met before the applicable solid line. Dissolution is then at the fast S_{max} rate in laminar flow at a slightly higher trend line slope of -0.250 log cm per log i, until the solid line is met at the limiting recharge point. Thereafter, slow high-order kinetics applies. For tubes longer than the coincidental lengths, the applicable solid line will be met first, indicating dissolution at slow high-order kinetics whilst still in transitional turbulent flow. This will slow down the dissolution rate significantly, taking more time to regain laminar flow. In both cases, the system would eventually reach a steady state with little change in parameters, except over long geological timescales.

An alternate outcome for the evolution of the 2y fissure or tube would arise if synchronous external valley deepening promotes vadose entrenchment at the resurgence. In time, this could lower the floor of the resurgence cave to the foot of the phreatic loop. The flow would then become entirely vadose, as in 2x above.

Reducing recharge conditions

Downward-trending conduits 3x behave similarly to 2x, except that, because Q is reducing, vadose entrenchment would become narrower, although the S_{max} dissolution rate should continue if saturation remains below 60%. If recharge ceases, any vadose flows would drain away at the resurgence, leaving a relict cave that descends from the upper to the lower entrance. This would consistently have an upper phreatic and a lower vadose morphology that records the previous flow regimes. An attempt to study breakthrough time under reducing recharge in such a conduit was made by Gabrovsek (2000, Fig. 1.3:3 and 44–45). His model of a hydraulic head that reduces exponentially with time apparently shows a delay to breakthrough or its absence, but does not recognize that flow would be vadose in these conditions. More generally, the modelling does not appear to include the complication caused by the original reduction in submerged length of a phreatic loop as the head reduces in vadose flow, and does not include the Reynolds Number in its treatment.

Conduits that form single phreatic loops 3y behave similarly to 2y, except that when the recharge starts to reduce, H, i, V and R_e will reduce more rapidly than under constant recharge. The relationship between i and conduit size would probably depend mainly on the way Q reduces rather than on the dissolutional enlargement. The effect on chemical breakthrough would be to increase the required w_B or r_B and delay T_B, but there would be little further reduction in L to reduce T_B. Thus, the kinetics cannot remain unchanged, and must move towards slower reaction rates.

For fissures, and comparing with 2y, $R_e = \rho Q/b\mu$ reduces proportionately with reducing Q, independently of the dissolutional widening, whereas $V = Q/bw$ reduces with both reducing Q and the increasing w. Hence, Q and V become insufficient to maintain the flow and chemical regimes that were already established under constant recharge. The fissure flow regime immediately starts to reverse back through its previous flow regimes, ultimately regaining laminar flow. Whilst still in fully turbulent flow, scallops would also lengthen as discussed for 2y, but at a faster rate, because V reduces faster. Similarly, the reaction kinetics also weaken as R_e reduces, and will also pass through a limiting recharge point at R_{eB} to regain slow high-order kinetic dissolution. Thus, these fissures follow similar events to those described for tubes in 2y, but perhaps more quickly, depending on the way Q and V reduce. This includes similar treatment for fissures shorter or longer than the coincidental lengths, except that, under reducing recharge, the system would probably reach a near-steady state sooner. In the limit, if recharge reduces to zero, the water becomes static. When visualizing fissure evolution under reducing recharge on Figure 1, if the fissure is in turbulent flow at the onset of reducing recharge, $w = (fQ^2/4\rho g b^2 i)^{1/3}$. Hence, because the w required to maintain turbulence reduces as $Q^{2/3}$ reduces, the slope of log w must be less steep than the -0.333 log cm per log i slope of the dashed lines. The new trend line will intersect the existing lines at points that indicate the hydraulic gradient and width at the changes back to transitionally turbulent then laminar flow at $R_{eF} = 30{,}360$ and $R_{eT} = 2200$. If the recharge reduces considerably, the trend line will approach the horizontal. When laminar flow is regained, $w = (12\mu Q/\rho g b i)^{1/3}$, and the slope of the trend line then increases slightly, because the required w now reduces as $Q^{1/3}$ reduces, but remains less steep than -0.333 log cm per log i. The visualization of the chemical behaviour for fissures shorter or longer than the coincidental lengths is similar to that for tubes 2y.

For tubes, $R_e = 2\rho Q/\pi r\mu$ reduces proportionately with both reducing Q and the increasing r, whereas $V = Q/\pi r^2$ reduces with both reducing Q and the increasing r^2. Hence, the new flow and chemical regimes reverse back faster than for tubes in 2y. This includes similar treatment and visualization on Figure 2 for tubes shorter or longer than the coincidental lengths, except that, under reducing recharge, the system would probably reach a near-steady state much sooner. Similarly, any scallops formed previously lengthen faster before fading away when $R_e < 24{,}860$ or $\lambda \geq 200$cm. If the tube is in turbulent flow at the onset of reducing recharge, $r = (fQ^2/4\pi^2\rho g i)^{1/5}$. Hence, because the required r reduces as $Q^{2/5}$ reduces, the slope of log r must be less steep than the -0.200 log cm per log i slope for tubes under constant recharge. The new trend line will intersect the existing dashed lines that have slopes of -0.333 log cm per log i at points that indicate the hydraulic gradient and radius at the reversals to transitionally turbulent then laminar flow. If the recharge reduces considerably, the trend line will approach the horizontal. When laminar flow is regained, $r = (8\mu Q/\pi\rho g i)^{1/4}$ and the slope of the trend line then increases slightly, because the required r now reduces as $Q^{1/4}$ reduces, but remains less steep than -0.333 log cm per log i.

As with 2y, another outcome for a fissure or tube could be vadose entrenchment at the resurgence, leading to the establishment of wholly vadose flow. Entrenchment would be narrower in this case, because Q is lower. Cessation of recharge would then leave a relict cave, as for 3x. If recharge ceases before the possible onset of wholly vadose flow, the conduit at the upper entrance would become relict above a static sump that may be perched above the base of a valley. This would either remain indefinitely, with only slow high-order dissolution maintained by slow convection currents, or it would eventually dry out by evaporation to create a relict phreatic loop.

Practical applications

The following sections discuss speleogenesis in common karst situations, mainly under hydraulic control. The recharge regime for each non-flooded karst system is determined by its effective local catchment area and its annual precipitation (P) less losses caused by evapotranspiration (E). A $1km^2$ catchment area with a P–E of 1m provides an annual recharge rate of $10^6 m^3 a^{-1}$, giving a mean flow rate of 32litres s^{-1}.

Diagenesis

Limestone is commonly formed by carbonate deposition in shallow tropical or deep marine environments, followed by compaction, lithification, and diagenesis in partly meteoric waters, with low hydraulic gradients under hydraulic control. During diagenesis, apertures are at the scale of the pores between crystals, which themselves may be <10microns in size. These are orders of magnitude below values in Figure 1 or 2, so that turbulence and chemical breakthrough do not apply.

Long drainage basins

Following exhumation and uplift, initial flows in homogeneous non-fractured limestone would be along inception horizons, perhaps in an adjacent more permeable lithology (Lowe and Gunn, 1997), but still with low hydraulic gradients. Apertures commonly remain at the pore scale, so that turbulence and breakthrough are still not possible initially, until high-order dissolution eventually creates conduits with w > 0.1cm. For example, long 'shallow' karst aquifers have $L \geq 1000$m and $i \leq 10^{-2}$. Transitional turbulence and chemical breakthrough do not occur there until a tube radius reaches 0.5cm and then >0.7cm. From Palmer (1991: Fig.13), this would take over one million years, if the initial aperture was 0.01cm, plus a delay because turbulence occurs first. Continuing enlargement under hydraulic control would next enable full turbulence and initial small scallop formation at $r_F = 2.7$cm. This would take only another 20 years. This value of r_F is close to the earlier example, where a tube with $r_F = 3.3$cm would not achieve dominant mechanical erosion until $r_M = 5$m. If hydraulic control persisted, this would take c. 5000 years. However, most such conduits would revert to at least a constant recharge flow regime. Thus, they, and conduits supplied from smaller catchment areas, would probably not reach dominant mechanical erosion.

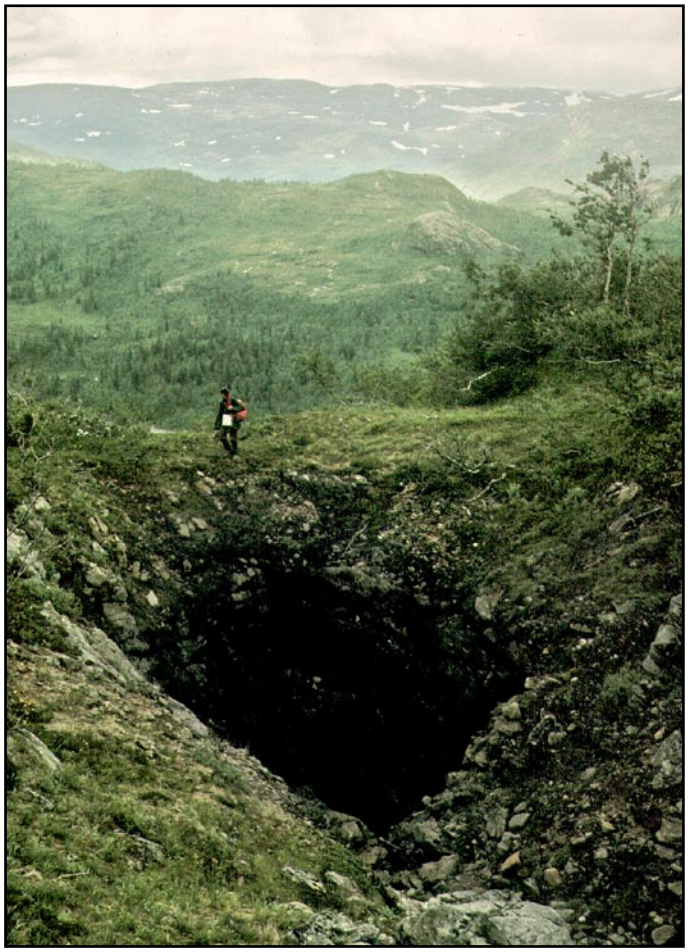

Figure 5: *Stream sinking just before reaching the side of the valley at Elgfjellelvgrotta, Norway.*

Shorter drainage routes

The initial radii of shorter shallow networks with 100m ≤ L ≤ 1000m and i ≤ 10^{-2} probably lie in the range 0.001–0.1cm. From Figures 1 and 2, these are not large enough to cause immediate transitional turbulent flow or chemical breakthrough. For steeper flows at i = 10^{-1}, breakthrough occurs at 0.15cm ≤ r_B ≤ 0.32cm, prior to or after the onset of transitional turbulence at r_T = 0.25cm, depending on conduit length. Continuing enlargement under hydraulic control could initiate (unseen) small scallop formation at r_F = 1.2cm. However, dominant mechanical erosion would occur at r_M = c. 5cm, which would take only c. 50 years. Thus, if such relatively steep fractures then enlarge under the same conditions to an enterable size before becoming relict and then being visited by cavers, no scallops will be observed. (If they remain sumped, divers would not enter them with V ≥ 300cm s^{-1}). This and the example immediately above illustrate the critical importance of the hydraulic gradient in controlling dominant mechanical erosion.

Tall vertical fractures

It is conceivable that limestone cliffs, including any ≥1000m high, could have flooded vertical fracture systems that reach from the cliff top to the cliff base. Water percolating down such fractures of any height at i = 1 would reach transitional turbulence at w_T = 0.17cm. For such a 1000m fracture, breakthrough occurs later at w_B > 0.25cm, if there is enough recharge to keep the fissure filled with water. For shorter cliffs, the required apertures for breakthrough are smaller, and breakthrough occurs before transitional turbulence in vertical fractures or tubes with heights smaller than 288–620m. These effects explain the numerous marble cave entrances located near valley shoulders in Central Scandinavia (Faulkner, 2005) (Fig.5). Full turbulence would occur at w_F = 1cm, but the dominant mechanical erosion flow velocity would occur first, for either a fissure or tube, preventing possible scallop formation. Hence if such fractures enlarge to explorable vertical shafts, no scallops will be observed that originated under constant head conditions. If the flow rate changes to constant or reducing recharge, the flow regimes will change to vadose, with headward mechanical and chemical erosion by a deep waterfall.

Epikarst joints and limestone pavements

In the epikarst, water-filled vertical joints ≤10m high could transmit water into a lower vadose zone under a constant head from local ponding. They would need apertures of only ≤0.06cm to achieve first-order kinetic dissolution, prior to transitional turbulent flow at w_T ≤ 0.17cm and the dominant mechanical erosion flow speed, prior to full turbulence at w_F = 1cm. This is the place where joint openings are naturally the largest, from surface stress relief and other processes. Hence, breakthrough and transitional and full turbulence are reached quickly here, or even immediately on the opening of a joint, if it is large enough for tectonic inception, and vadose flow may follow soon after. This explains the epikarst phenomenon, where cave entrance passages can be showered with water during heavy rain. Similarly, new dolines can form rapidly in abandoned limestone quarries (Gunn and Gagen, 1987). Because dominant mechanical erosion effectively occurs at w_M = 2cm, small scallops would not form. Vertical grikes c. 1m deep are common in limestone pavements. They achieve fast dissolution with apertures of only ≤0.025cm, making tectonic inception even more likely here. However, if the epikarst and/or the limestone pavement do not remain flooded, these environments are likely to support a constant recharge regime, when averaged over several years, giving vadose flows down the joints. Smooth pavements under continuous cold rainfall would lower up to 0.5mm per year by dissolution, best exemplified by 1.5m of vertical marble erosion in the Holocene at Madre de Dios, Chile (Faulkner, 2009b).

Speleothem dripwaters

Speleothem deposition occurs when dissolved calcite precipitates by CO_2 vigorously degassing in cave air, where the dripwater flow reaches an open passage roof or wall. If autogenic water at 10°C seeps through a non-carbonate rock with P_{CO2} of 1% derived from overlying soils, it will contain little dissolved calcite before entering the limestone, but will then reach calcite saturation in closed conditions at 50mg per litre (Palmer, 1991: Fig.7). Similar autogenic water flowing through calcareous soils with 1% P_{CO2} continuously maintained in open conditions could saturate at 212mg $litre^{-1}$ before entering the limestone. The P_{CO2} of cave air does not normally fall below its level in the surface atmosphere, presently 0.04%. Water under such conditions saturates at 12 or 68mg $litre^{-1}$ in closed or open conditions, respectively. Assuming degassing occurs under open conditions, drips may thus become aggressive and capable of dissolving 18 mg $litre^{-1}$, with no deposition, or deposit a maximum of 144mg of speleothem from each litre of water. Water flowing from a passage via fissures in its floor that drips into a lower passage may experience "prior calcite precipitation" (PCP: Fairchild and Baker, 2012, p.26). It will then become aggressive if the P_{CO2} of the cave air in the lower passage is higher, or alternatively deposit speleothem again.

It seems conceivable that dripwaters could achieve chemical breakthrough and then enlarge bedding planes and joints along their flow path and re-dissolve previously deposited speleothem, eventually creating explorable passages and shafts. However, the presence of large and old speleothems in many caves, without signs of corrosion, suggests that dripwaters commonly enter the limestone nearly saturated and/or flow in long tiny fissures, and/or exhibit constant or reducing recharge conditions, whilst remaining near, or approaching closer to, saturation for >>100,000 years. In the competition between the slow enlargement of the dripwater flow path and the lower P_{CO2} level of cave air, degassing should help retain the chemical regime before the drip exit in a pre-breakthrough condition and prolong deposition. However, the rarer presence of corroded speleothems in some caves shows that the breakthrough point can be reached locally.

The geometry of dripwater flow paths is never known, and has rarely, if ever, been modelled. Cave air P_{CO2} can vary from dangerous levels of ≈5%, when degassing and deposition are unlikely, to atmospheric levels at cave entrances, where speleothems are occasionally located. Nevertheless, dripwaters from cave roofs that follow a vertical path down short joints from a bare limestone surface are more likely to be aggressive and less likely to deposit speleothem, in contrast to those that flow from calcareous soils along longer flow paths with small hydraulic gradients. Under intermediate conditions, dripwaters might become aggressive during floods that raise hydraulic gradients, thereby causing dissolution of speleothem.

During winter, interesting and complex competitions arise among the effects of lower temperature and its consequential reduction of biological activity and therefore of P_{CO2} in dripwaters. Reduced temperature increases the amount of calcite that can be held in solution, thereby increasing penetration lengths and significantly reducing breakthrough times. Reduced P_{CO2} levels reduce the calcite saturation level, thereby reducing penetration lengths and increasing breakthrough times. After breakthrough, maximum dissolution rates are reduced towards 0.35mm a^{-1} at 0°C and low P_{CO2} (Faulkner, 2006a). Because the temperature change is likely to be damped when the dripwater reaches open cave passage, the change in P_{CO2} is likely to have the major influence. Thus, assuming the dripwater flow always operates with high-order kinetics, i.e. it remains nearly saturated and pre-breakthrough, its solute load is reduced and therefore winter precipitation of speleothem should be reduced at the same flow rate, unless the P_{CO2} of winter cave air also reduces.

Speleogenesis below high-level reservoirs and lakes

If the entry to the karst is itself under a head of water, this head must be added to the head within the karst to give the applicable hydraulic gradient, if the discharge is into a lower valley. Such increased hydraulic gradients can cause rapid breakthrough by enlargement of karst fractures beneath a reservoir, as studied by Dreybrodt (1996): an extreme example of hydraulic control. Thus, a reservoir dam can be bypassed by an underlying conduit, causing significant leakage of the reservoir. Close to the wall of the dam, i can exceed unity. For example, from Figure 1, if the leakage is 900m away and down the valley from a fracture system that leads 100m below the base of a dam that holds back water 100m deep, L = 1000m and i = 200/1000 = 0.2. Transitional turbulence occurs at w_T = 0.3cm, breakthrough at w_B > 0.4cm and full turbulence at w_F > 1.4 cm. For a 10m-long sub-horizontal fracture directly beneath the same dam, i = 10, giving a breakthrough aperture of 0.025cm, and transitional and full turbulence at w = 0.08 and 0.38cm, so that immediate tectonic inception is likely here. Similar conditions arose during the Weichselian deglaciation of continental ice sheets in mountainous areas, when the fractures become submerged by ice-dammed lakes (Faulkner, 2008). In this case, the flow path is from the lake and via the fractures back into the lake and then into englacial conduits within the continuing ice sheet, or directly from the fractures into Nye channels at the base of a warm-based ice sheet, or directly via the fractures into an adjacent ice-free valley. Despite the water being at 0°C, with a P_{CO2} then of only 0.02%, such situations can also cause tectonic inception and first-order dissolution at the fairly rapid rate of 0.35mm a^{-1} (Faulkner, 2006a).

Rejuvenation in alpine situations

Glacial valleys in mountainous areas, including those at high latitudes, were significantly rejuvenated following large-scale erosion during each Pleistocene glaciation. At least the upper and outer parts of palaeocaves may be removed during glacial maxima (Faulkner, 2008). During each ensuing interglacial, sinks may be captured farther upstream and resurgences find lower outlets. Clearly, these effects may make significant changes to hydraulic gradients and hydraulic ratios, depending on the local topography. They provide opportunities for new fractures at lower levels to carry some of the interglacial drainage. These may in turn eventually achieve transitional turbulent flow and chemical breakthrough and then grow large enough under fully turbulent flow and/or dominant mechanical erosion to be explored by diving, after a return to catchment control.

Drainage routes in marble karst

Limestone that has been metamorphosed at least to medium grade amphibolite facies marble commonly retains no porosity related to its original structure. Thus, any karstification deriving from inception horizons in its earlier sedimentary environment is lost and its new primary porosity is too low to permit significant pre-breakthrough dissolution in the geological time available. Instead, speleogenesis in such marble relies on the creation of fractures in phreatic conditions by various tectonic and uplift processes during erosion of the landscape, especially where these have been amplified by cycles of glaciation and deglaciation (Faulkner, 2005, 2006a, 2006b, 2008, 2009a). The foliation and structural dip of these marbles is commonly steep, frequently vertical and rarely horizontal, with fractures following planes that are parallel to and orthogonal to the foliation. Consequently, hydraulic gradients vary from the near-horizontal, where water flows along joint planes orthogonal to vertical foliation, to the near-vertical, where allowed by the topography. However, flow path lengths are commonly short, averaging only tens of metres, and never exceed a few kilometres. Thus, from Figure 1 or 2, laminar flow and high-order kinetic dissolution may be bypassed in many such environments by tectonic inception along fractures with millimetre-scale apertures. Many of these systems have steep hydraulic gradients, causing high flow rates, so that small scallops formed under fully turbulent flow are quite common (Fig.4), as is the effect of normal mechanical erosion.

Conduit morphology

In phreatic conditions, and after turbulence and chemical breakthrough, conduits and cave passages tend eventually to become circular in cross-section, unless their floors become armoured by clastic sediment. (In that case, paragenetic dissolution is predominantly upwards). This is because stream velocity and mechanical erosion are highest near the centre of an originating planar fracture (which will pass through an elliptical form) or at the centre of a junction of fractures (which may be circular initially). The probability of achieving circular cross-section increases with the time available and in the order: reducing recharge, constant recharge and constant head conditions. There is no transition to vadose flow under constant head conditions, and the passage should continue to enlarge with an ultimate circular cross-section. If the phreatic to vadose transition occurs in constant recharge conditions, then the vadose part of the passage should have the same width as the upper phreatic part. In gradually reducing recharge conditions, these passages commonly have a distinctive V-shaped morphology below a phreatic roof section, indicative of a water level that has gradually lowered in reducing flow below an air space. An example of probable gradually reducing recharge is provided by the many relict passages in Jeskyne na Spicaku in the Czech Republic (Fig.6). The more normal keyhole cross-section at the phreatic / vadose junction is indicative of a sudden reduction in flow rate synchronized with, or perhaps succeeded later by, the advent of vadose flow. Relict phreatic passages without a vadose trench indicate that the flow to that passage was suddenly cut off and did not return. The water in the passage then either drained away or was left as a perched sump, which later dried out by evaporation.

Sumps

The hydrogeological characteristics of sumped passages can be derived from Figure 2. All sumped passages, from the smallest that can be dived into, with L ≤ 10km, r ≥ 25cm, f = 0.029 and i ≥ $2x10^{-6}$ (giving V ≥ 2.5cm s^{-1} from the D-W equation) always enlarge phreatically at the S_{max} rate under fast first-order dissolution kinetics in turbulent flow (reached earlier when r ≥ 9cm). So do those with L ≤ 1km, r ≥ 25cm and i ≥ $2x10^{-7}$ (giving V ≥ 0.8cm s^{-1} and earlier turbulent flow when r_T ≥ 20cm); or with L ≤ 100m, r ≥ 25cm and i ≥ $2x10^{-8}$ (giving V ≥ 0.3cm s^{-1} and later turbulent flow when r_T ≥ 50cm). Thus, in nearly all practical cases, sumps explored by diving continue to enlarge at S_{max}, providing that the inflowing water at the start of the sump has a negligible concentration C_0 of calcite. The S_{max} rate is likely at high stage near a sink, but may be less likely at low stage near a resurgence. These characteristics are based on values of hydraulic gradient and so apply to all flow regimes. However, if i reduces under catchment control or reducing recharge conditions, then the limiting recharge point could be reached, before or after a return to laminar flow, especially at low stage. Thereafter, enlargement is constrained by slow high-order kinetics, the outlet water is almost saturated with calcite, and enlargement eventually ceases.

Scallops

Scallops in relict passages indicate the final flow direction and velocity at high stage in fully turbulent flow at R_e ≥ 24,860, with dissolution most likely utilizing first-order kinetics, prior to the passage being drained or drying out by evaporation. This dewatering could occur after any recharge regime. If any passage under constant head, or a planar fissure under constant recharge, suddenly becomes relict, scallop lengths represent the fastest flow velocity achieved. However, when a cylindrical tube under constant recharge, or any passage under

Figure 6: *Passage profile, in Jeskyne na Spicacu, in the Czech Republic, illustrating the gradual transition from phreatic to vadose conditions under reducing discharge.*

Figure 7: *A wedged granite boulder in Grønligrotta, Norway. It was probably transported into the cave by a jökulhlaup when a local ice-dammed lake collapsed during deglaciation (photo: Shirley St Pierre).*

reducing recharge, becomes relict, previous flow velocities would have been higher than recorded by any final scallops. The absence of scallops in explorable cylindrical relict phreatic passages ($r \geq 15$cm) infers one of:

a) In passages with (w/2 or r) < 200cm at low i, fully turbulent flow had never been reached, even at high stage under constant head conditions;

b) In larger passages with (w/2 or r) ≥ 200cm at low i under constant head conditions, the final high stage velocity <1cm s^{-1} was still not large enough for recognizable scallops to form with $\lambda < 200$cm, even at full turbulence;

c) In long passages at low i, chemical breakthrough had not occurred.

d) The final flow regime was fast enough at $V \geq 162$cm s^{-1} for dominant mechanical erosion to erase previous scallops at a minimum length of λ = c. 1cm.

e) The passage became relict after a prolonged period of reducing recharge for any passage or constant recharge if a tube, so that R_e became <(30,360 or 24,860) and/or the flow velocity fell to <1cm s^{-1} at $\lambda = 200$cm, when any previous scallops faded away by dissolution, probably before the limiting recharge point was reached.

Scallops in tubes with r < 15cm may not be observed directly and there are no known references to studies of scallops observed at the entries of such conduits into explorable cave passages. If a diver enters a sump at high stage, the lengths of any observed scallops should represent the flow velocity near the conduit wall. Scallops with $\lambda \geq 3$cm should be recognizable. If scallops are seen with $\lambda < 3$cm during low stage, these would have formed when $V > 100$cm s^{-1}, which is probably too fast to permit diving.

High flow rates

Examples of palaeo high speed flow in caves are provided by many erratic granitic gneiss boulders that are wedged in the roofs of passages in Grønligrotta, Norway, within 100m of the cave entrances (Fig.7). They typically measure up to one metre in size and, from a Hjulström diagram, it required a flow velocity ≥200cm s^{-1} to transport such boulders before they jammed. This was probably caused by a jökulhlaup when a local ice-dammed lake collapsed during deglaciation. In places, smooth walls with a complete absence of scallops might indicate dominant mechanical erosion and that the velocity was probably much higher than 200cm s^{-1}. The large scallops in Figure 7 were either created in slower moving water before the jökulhlaup event, which probably lasted for several hours, but were not all removed by it, or they were formed if and when the cave remained flooded after the event.

As another extreme example of possible scallop removal during conduit enlargement, the largest underground river in Europe is along the Trebisnjica river basin in the Dinaric karst of Croatia (Bonacci, 2013). It has an annual mean discharge of 28m^3s^{-1} from a catchment area of c. 1000km^2 and a flow velocity of 34km in 5 days (Zubac, 2013 and presentation), from an altitude of 260m down to near sea level. Approximating, these figures give $i = 8x10^{-3}$ and $V = 8$cm s^{-1}. Assuming that only a phreatic circular conduit is applicable in these conditions, $Q = \pi r^2V = 28m^3s^{-1}$, so that r = c. 10m. However, the Trebisnjica Spring has a peak discharge of $Q = 800m^3s^{-1}$, giving a peak flow mean conduit velocity $V = 250$cm s^{-1} and $R_e = 3.8x10^7$ at 10°C. The friction factor $f = 4rgi/V^2 = 0.5$ suggests some partial blockages along the flow path. Because $V < V_\lambda$, the velocity only 1cm from the conduit wall that is required to remove scallops, dominant mechanical erosion does not appear to be reached, even in this conduit. Indeed, at its scallop demise, $r/\lambda = 1000$, giving λV = c. 700 cm^2s^{-1}, so that a mean velocity of $V = 700$cm s^{-1} would be needed to remove scallops, suggesting that scallops may still exist.

Conclusions

If speleogenesis has sufficient time for conduit development to proceed under hydraulic control (constant head), catchment control (constant recharge), then reducing recharge conditions, it will commonly follow the principles and steps summarized below and presented in Table 2.

1

The onset of transitional and then full turbulence in a uniform conduit under hydraulic control is governed by two main variables: the aperture (i.e. fissure width or tube radius) and the hydraulic gradient, whereas the onset of first-order kinetics at chemical breakthrough is also controlled by the length of the conduit. Mathematically, hydraulic gradient and length are usefully combined into a single variable, the hydraulic ratio, which equals the hydraulic gradient divided by the conduit length. Many karst aquifers have path lengths of 100–1000m at hydraulic gradients from 10^{-4} to 10^{-2}. From Figure 1 or 2, the breakthrough point in a 100m-long fissure or tube occurs when the aperture or radius reaches 0.54–2.51cm or 0.32–1.50cm over this range of i. For 1000m- and 10000m-long flow routes, the required sizes increase to >1.17–5.41cm or >0.70–3.24cm and >2.51–11.66cm or >1.50–6.97cm. However, for steep flows with $10^{-2} \leq i \leq 10^{0}$, they can reduce to <1mm. For long flow paths with $i \leq 10^{-4}$, they can increase up to several metres.

2

As a conduit enlarges by dissolution, the onset of transitional turbulence occurs at a probable maximum Reynolds Number $R_{eT} = 2200$, whereas at chemical breakthrough at the onset of first-order kinetics, R_{eB} is proportional to the conduit length L. The two onsets only coincide if L = 288–620m (when $R_{eT} = 3.55L–7.65L$), depending on conduit shape and ambient temperature, the actual aperture depending on the hydraulic gradient. Thus, breakthrough may occur before or after flow becomes transitionally turbulent, depending on conduit length being shorter or longer than the coincidental length. For shorter conduits, this has no impact on existing models of karstification, because the size needed for transitional turbulence is reached quickly by dissolution under fast first-order kinetics at a fast laminar flow rate. For longer conduits, and especially those longer than 1000m at hydraulic gradients $<10^{-6}$, the prior onset of turbulent flow could increase the minimum conduit size needed for breakthrough, perhaps significantly increasing modelled breakthrough times and reducing the extent of karstification.

3

After breakthrough, fissure width or tube radius increases linearly with time at the S_{max} rate, depending only on temperature and P_{CO2}. R_e increases at an accelerating rate until R_e = (30,360 or 24,860) at the onset of fully turbulent flow, when the conduit size has increased by a factor of (5.75 or 5.04) from its size at the onset of transitional turbulence. Thereafter, wall scallops can start to form, at an initial length equal to the half-width or radius of the conduit.

4

For many practical conduits, including those with L < 10km at a hydraulic gradient $i > 10^{-4}$ or L < 1km at $i > 10^{-6}$, breakthrough occurs before or soon after full turbulence is reached, so that most observed scallops formed when flow was fully turbulent and the conduit walls were dissolving at the applicable S_{max} rate.

5

Conduit size increases further and scallop lengths reduce as the flow rate and velocity continue to increase, until the mean velocity V reaches c. 300cm s^{-1}. Mechanical erosion then dominates over chemical dissolution and scallops start to disappear at their minimum size of c. 1cm. However, with realistic recharge rates, this process can only remove scallops that were formed in small conduits; at large hydraulic gradients it prevents the formation of scallops.

6

The above scenario for conduit evolution wholly under hydraulic control applies to a restricted set of global karst systems, including those that were initiated by tectonic inception and then flooded under a reservoir or during deglaciation. Normally, the recharge regime changes later from a constant head condition to constant recharge and then to reducing recharge.

7

At the onset of constant recharge conditions, downward-trending conduits evolve by vadose entrenchment. Planar fissures that remain sumped below resurgence level become locked into their new flow and chemical regimes at a constant R_e in perpetuity, or at least until their cross-sections become more circular. Their width increase by either fast first-order dissolution kinetics or slow high-order kinetics is balanced by the consequential reduction in velocity. Cylindrical tubes sumped below resurgence level immediately start to reverse back through their previous flow regimes towards laminar flow and reverse back towards high-order dissolution kinetics via the limiting recharge point. For both sumped fissures and tubes, any scallops formed could lengthen until they become unrecognizable at λ = 200cm when V = c. 1cm s^{-1}.

8

At the onset of reducing recharge, downward-trending conduits continue to evolve in vadose conditions, but with narrower entrenchments, until they become relict if recharge ceases. All conduits that remain sumped below resurgence level immediately start to reverse back through their flow and chemical regimes at a faster rate than under constant recharge. If recharge ceases, the sumps either remain static or dry out by evaporation.

Thus, there are many different situations governed by the same laws that cause widely differing karst characteristics and timescales. In practice, the conduit sizes for transitional and full turbulence and breakthrough may vary from the sub-millimetre to several metres and hydraulic ratios can be considered over 17 orders of magnitude. By considering the likely recharge conditions, the flow and chemical regimes, and the conduit geometry that each epigenic cave experienced as its local topography evolved, its total history from chemical or tectonic inception to its present morphological and hydrogeological condition should be realizable.

Acknowledgements

The author is grateful to Philippe Audra, Franci Gabrovsek, Art Palmer and Steve Worthington for their suggestions that led to the improvement of several points in the paper or its earlier versions; and especially to Rane Curl for providing clarification of the various Reynolds Numbers to be used in the consideration of scallop morphology and development, thereby enabling a more rigorous analysis.

References

Blumberg, P N and Curl, R L, 1974. Experimental and theoretical studies of dissolution roughness. *Journal of Fluid Mechanics*, Vol.65(4), 735–751.

Bonacci, O, 2013. *Possible negative consequences of underground dam and reservoir construction in coastal karst area: example of HEPP Ombla near Dubrovnik, (Croatia).* p.52 *in* Madl-Szonyi, J, Eross, A, Mindszenty, A and Toth, A (eds), *International Symposium on Hierarchical Flow Systems in Karst Regions.* Symposium program and abstracts, 4–7 September 2013, Budapest.

Bögli, A, 1964. Mischungskorrosion – ein Beiträg zur Verkarstungsproblem. *Erdkunde,* Vol.18, 83–92. [English translation provided by Elder, E, 1985. Mixture Corrosion – a contribution to the karstification problem. *National Speleological Society, Cave Geology,* Vol.1(10), 393–406.]

Curl, R L, 1966. Scallops and flutes. *Transactions of the Cave Research Group of GB*, Vol.**7** 121–160.

Curl, R L, 1974. Deducing flow velocity in cave conduits from scallops. *National Speleological Society Bulletin,* Vol.36(2) 1–5.

Dreybrodt, W, 1988. *Processes in Karst Systems: Physics, Chemistry and Geology.* [New York: Springer.] 255pp.

Dreybrodt, W, 1990. The role of dissolution kinetics in the development of karst aquifers in limestone: a model simulation of karst evolution. *Journal of Geology,* Vol.98(5), 639–655.

Dreybrodt, W, 1996. Principles of early development of karst conduits under natural and man-made conditions revealed by mathematical analysis of numerical models. *Water Resources Research,* Vol.32(9), 2923–2935.

Dreybrodt, W, Gabrovsek, F and Romanov, D, 2005. *Processes of speleogenesis: a modeling approach*. [Postojna–Ljubljana: Zalozba, ZRC.] 376pp.

Fairchild, I J and Baker, A, 2012. *Speleothem Science.* [Wiley-Blackwell.] 432pp.

Faulkner, T, 2004. Scallops and dissolution rate. *Cave and Karst Science*, Vol.31(1). [Forum:] 43–44.

Faulkner, T L, 2005. *Cave inception and development in Caledonide metacarbonate rocks*. PhD Thesis. University of Huddersfield, UK.

Faulkner, T, 2006a. Limestone dissolution in phreatic conditions at maximum rates and in pure, cold, water. *Cave and Karst Science*, Vol.33(1), 11–20.

Faulkner, T, 2006b. Tectonic inception in Caledonide marbles. *Acta Carsologica,* Vol.35(1), 7–21.
Faulkner, T, 2007. Book review: Hypogene Speleogenesis: Hydrogeological and morphogenetic perspective by Dr A B Klimchouk, National Cave and Karst Research Institute Special Paper No. 1, 2007, 106pp. *Cave and Karst Science,* Vol.33(3), 138–141.
Faulkner, T, 2008. The top-down, middle-outwards model of cave development in Caledonide marbles. *Cave and Karst Science,* Vol.34(1), 3–16.
Faulkner, T, 2009a. The endokarstic erosion of marble in cold climates: Corbel revisited. *Progress in Physical Geography,* Vol.33(6) 805–814.
Faulkner, T, 2009b. Limestone erosion rates and rainfall. *Cave and Karst Science,* Vol.36(3), 94–95.
Faulkner, T, 2013. How do the aperture sizes in limestone vary for the onsets of turbulent flow and first-order dissolution kinetics? *Proceedings of the Sixteenth International Congress of Speleology,* Vol.3, 349–355.
Ford, D C and Williams, P, 2007. *Karst hydrogeology and geomorphology.* [Chichester: John Wiley and Sons.] 562pp.
Gabrovsek, F, 2000. *Evolution of early karst aquifers: from simple principles to complex models*. [Ljubljana: Zalozba ZRC.] 150pp.
Gunn, J and Gagen, P, 1987. *Limestone quarrying and sinkhole development in the English Peak District.* 121–125 *in* Beck, B F and Wilson, W L (eds), *Karst Hydrogeology.* [Rotterdam: Balkema.]
Hanna, R B and Rajaram, H, 1998. Influence of aperture variability on dissolutional growth of fissures in karst formations. *Water Resources Research*, Vol.34(11) 2843–2853.
Kaufmann, G and Braun, J, 1999. Karst aquifer evolution in fractured rocks. *Water Resources Research,* Vol.35(11), 3223–3238.
Kaufmann, G, 2003. Modelling unsaturated flow in an evolving karst aquifer. *Journal of Hydrology*, Vol.276(1–4), 53–70.
Klimchouk, A, 2007. *Hypogene Speleogenesis: Hydrogeological and Morphogenetic Perspective.* National Cave and Karst Research Institute Special Paper No.1. 106pp.
Lowe, D J and Gunn, J, 1997. Carbonate Speleogenesis: An Inception Horizon Hypothesis. *Acta Carsologica*, Vol.26/2, 38, 457–488.
Palmer, A N, 1981. Hydrochemical factors in the origin of limestone caves. *Proceedings of the Eighth International Congress of Speleology: Bowling Green, Kentucky, U.S.A., July 18 to 24, 1981,* 120–122.
Palmer, A N, 1991. Origin and morphology of limestone caves. *Geological Society of America Bulletin,* Vol.103, 1–21, 157–175.
Palmer, A, 2007. *Cave Geology*. [Dayton, Ohio: Cave Books.] 454pp.
Plummer, L N, Wigley, T M L and Parkhurst, D L, 1978. The kinetics of calcite dissolution in CO_2 – water systems at 5° to 60°C and 0.0 to 1.0 atm. CO_2. *American Journal of Science,* Vol.278 179–216.
Romanov, D, Gabrovsek, F and Dreybrodt, W, 2003. The impact of hydrochemical boundary conditions on the evolution of limestone karst aquifers. *Journal of Hydrology,* Vol.276, 240–253.
Weyl, P K, 1958. The solution kinetics of calcite. *Journal of Geology,* Vol.66, 163–176.
White, W B, 1977. *Role of solution kinetics in the development of karst aquifers.* 503–517 *in* Tolsen and Doyle (eds), *International Association of Hydrogeologists, Memoirs,* 12.
White, W B, 1988. *Geomorphology and hydrology of karst terrains*. [Oxford University Press.]
Zubac, Z, 2013. *Multipurpose system of hydropower plants on the river Trebisnjica.* p.148 *in* Madl-Szonyi, J, Eross, A, Mindszenty, A and Toth, A (eds), *International Symposium on Hierarchical Flow Systems in Karst Regions*. Symposium program and abstracts, 4–7 September, 2013, Budapest.